Machine Vision Based Automatic Quality Inspection System for Connecting-rod

Nadia Riaz Bajwa

Regn Number

NUST201362029MSMME62113F

Supervisor

Dr. Syed Irtiza Ali Shah

Co-Supervisor

Dr. Syed Omer Gillani

SCHOOL OF MECHANICAL & MANUFACTURING ENGINEERING

NATIONAL UNIVERSITY OF SCIENCES AND TECHNOLOGY

ISLAMABAD

JUNE, 2017

Machine Vision Based Automatic Quality Inspection System for Connecting-rod

Author

Nadia Riaz Bajwa

Regn Number

NUST201362029MSMME62113F

A thesis submitted in partial fulfillment of the requirements for the degree of

MS Robotics and Intelligent Machine Engineering

Thesis Supervisor:

Dr. Syed Irtiza Ali Shah

Thesis Co-Supervisor

Dr. Syed Omer Gillani

Thesis Supervisor's Signature: _____

SCHOOL OF MECHANICAL & MANUFACTURING ENGINEERING

NATIONAL UNIVERSITY OF SCIENCES AND TECHNOLOGY,

ISLAMABAD

JUNE, 2017

Declaration

I certify that this research work titled "*Machine Vision-based Automatic Quality Inspection System for Connecting-rod"* is my own work. The work has not been presented elsewhere for assessment. The material that has been used from other sources it has been properly acknowledged / referred.

Signature of Student

Nadia Riaz Bajwa

NUST201362029MSMME62113F

Plagiarism Certificate (Turnitin Report)

This thesis has been checked for Plagiarism. Turnitin report endorsed by Supervisor is attached.

Signature of Student

Nadia Riaz Bajwa

Registration Number

NUST201362029MSMME62113F

Signature of Supervisor

Copyright Statement

Acknowledgements

I am thankful to my Creator Allah Subhana-Watala to have guided me throughout this work at every step and for every new thought which You setup in my mind to improve it. Indeed I could have done nothing without Your priceless help and guidance. Whosoever helped me throughout the course of my thesis, whether my parents or any other individual was Your will, so indeed none be worthy of praise but You.

I am plentiful grateful to my cherished parents who raised me when I was not fit for strolling and kept on supporting me all through in each period of my life. Words cannot express how grateful I am for all of the sacrifices that you people have made on my behalf. Your prayer for me was what sustained me thus far.

Foremost, I would like to express my sincere gratitude to my supervisor Dr. Syed Irtiza Ali Shah for the continuous support of my MS study and research, for his patience, motivation, enthusiasm, and immense knowledge. His guidance helped me in all the time of research and writing of this thesis. I could not have imagined having a better advisor and mentor for my thesis.

I would like to thank my Co-supervisor, Dr. Syed Omer Gillani, for the patient guidance, encouragement and advice he has provided throughout my time as his student. I have been extremely lucky to have a Co-supervisor who cared so much about my work, and who responded to my questions and queries so promptly.

Besides my advisors, I would like to thank the rest of my thesis committee: Dr. Yasar Ayaz, Dr. Syed Omer Gillani and Dr. Naveed, for their encouragement and insightful comments.

I am also indebted to my friend Hafsah, who comes up with critical questions and constructive advice to improve my thesis. Furthermore, I have to offer my special thanks to my dearest friend Oaj e Surrayya, she helped me when I encounter any difficulties in writing and she used to correct my endless grammatical mistakes.

Dedicated to my exceptional parents and adored siblings whose tremendous support and cooperation led me to this wonderful accomplishment

Abstract

This research deals with attempting to study, analyse, design, implement and testing of automatic machine vision-based system for quality control of engine Connecting-rod. The connecting-rod or conrod links the piston, which is a part of reciprocating engine, to the crankshaft. In combination with crankshaft, connecting-rods convert up and down motion of piston into rotating motion. In industries, large number of connecting rods with different diameters are being manufactured for various engines. Usually parameters of conrod such as large bore diameter are measured manually by using different gages. In this method, human mistakes contributes to for inaccurate diameter measurement. As automatic quality inspection system for connecting-rod is proposed to estimate its large bore diameter and small bore diameter of different sizes using machine vision. In order to measure the parameters of connecting-rod, both methods Circular Hough transform and Histogram Based Edge Detection have been implemented and compared. However satisfactory results have been achieved with Histogram Based Edge Detection. The proposed algorithm provides accuracy, efficiency and it is also cost-effective as compared to existing manual inspection system.

Table of Contents

List of Figures

List of Tables

List of Symbols

SNR	Signal-to-Noise Ratio
CHT	Circular Hough Transform
RGB	Red Green Blue
HBED	Histogram Based Edge Detection
SAR	Synthetic Aperture Radar
LOG	Laplacian of Gaussian
IAT	Image acquisition Toolbox
DSLR	Digital Single Lens Resolution

CHAPTER 1: INTRODUCTION

1.1 Literature Review

In manufacturing quality inspection is a noteworthy perspective. Tiredness and tediousness are main factors of human involved functioning which effect productivity and efficiency. Concentrated on fulfilling the quality prerequisites of both the customer and the manufacturer. Quality Control take part as main role in all industrialised surroundings, together with checking of components [1]. Quality demands for manufacturing goods like piston, crankshaft screw, connecting-rod and some parts of auto motor are characterized by standard pictures for the goods. Inspecting the quality of manufacturing goods manually is a very difficult task. It takes long time to control visually and inspection of specialist for the parts moreover it is not sufficiently precise, along these lines of fault identification is extremely subject to failures [2]. So, the goal is to lessen manufacturing expenses due to human involvement in the fault investigation or due to the rejection of malfunctioning goods by certifying reliable manufactured article quality.

A few methodologies are feasible for autonomous checking of production assembly, for example, vision-based methodologies and weight estimation based methodologies. Be that as it may, a few requirements ought to be considered to settle on the best decision. To start with, changes made in the current assembly process ought to be minimized. Changing the current assembly process may force a critical danger for the organization; rather, another technique for autonomous checking ought to be converged with the present assembly process with least changes to the present procedure. Consequently, the minimum possible measure of alterations of the assembly should be focused on. Second, the new checking technique ought to be acquainted without broad changes with equipment to minimize extra costs that the new strategy may require [3]. Third, the new strategy ought to make preferable effectiveness over the present manual technique. Most extreme proficiency ought to be accomplished contrasted and the manual procedure by the new strategy. Machine Vision based methodology is considered in this work. Currently, parameter estimation of each item of connecting rod is done from the images taken from the digital single-lens reflex camera. Next, the images are prepared to obtain data for checking. In this phase, the only hardware needed for this methodology is cameras. Also, the software required for image processing are effectively combined with the present production process. This vision-based methodology can fulfil the initial two requirements and is relied upon to fulfil the third limitation in light of the fact that a considerable measure of vision-based techniques have been

connected to different procedure checking tasks and have highlighted the accomplished productivity contrasted and that of manual work.

The developing strategies for robotized visual checking depend on systems of Machine Vision. Uses of machine vision systems for the most part expand the effectiveness, quality and the efficiency of procedure mechanization and subsequently are profited to the prudent variables of a manufacturing firm. Machine vision is the learning and methodologies used to give image based programmed examination to quality control, process control, and robot direction. Essentially machine vision is utilized for optical gaging, quality assurance, sorting, part get together investigation, nearness and default and controlling the assembling procedure. Machine Vision system operation begins with procurement of an image utilizing suitable cameras, lenses and light contingent upon the application. The computerized image can be utilized as a part of machine vision in numerous applications. There are numerous algorithms to separate the different attributes from the image autonomously. A standout amongst the most vital application on image is identification and order different sorts of faults in digital image. Softwares like MATLAB, OpenCV, MV Impact, labVIEW will give various digital images preparing strategies utilized for getting required data from a procured digital images. In light of the extricated image the processor will take choice i.e. passable or impassable. Along these lines NOT worthy segment will be expelled from the assembly line utilizing discharge instrument, for example, blower or actuator [4].

After capturing images from camera three steps are mainly followed to get desired results. In the first step image is segregated into multiple segments to acquire something more meaningful. Basically image is stored in the form of pixels and to give label to all pixels in an image is the purpose of its segmentation. So, the pixels having same labels sharing some definite features. In the second step feature extraction needs to be done for object detection and recognition. In the third step after extracting useful features, the task is to identify objects in an image. This thesis deals with the parameter estimation of connecting rod such as large bore diameter and small bore diameter using machine vision methodology in order to build a quality inspection for the conrod. To estimate these parameters of connecting-rod first Gradient based Circular Hough Transform is used. The results acquired by using this method is not accurate enough. By using this method diameters of both circles were measured in number of pixels, but when no of pixels were converted to millimetres, result went beyond the tolerance range, due to which Histogram Based Edge Detection Method has been used. The approach is derived on calculating the distance transform between edge pixels and all the pixels in the image. To get the number of occurrences of the

distances that play apart in the accumulator space that consists from votes, histogram is used. For the detection of distinct sizes of circle, single accumulator space is used.

1.2 Segmentation:

The process of reducing processing complexity by examining only region of interest in the image is known as image segmentation. It can also say that it is an attempt to extract meaningful information from the “background” as “background” is made up of those regions of the image that do not deliver information to accomplish the desired task.

Segmentation suggests an advanced level explanation of the image which is given by the original gray level pixels. It splits the raw image into diverse regions that can be characterised by features except the gray levels. Such features are known as parameters.

A basic thresholding operation might be utilized if picture is a scene with luminescence brightening where bright objects cast dim shadows, and our objective is to remove the shadow areas. We may handle by selecting a threshold, such as gray level is established up to which all the gray levels in the image matched. At that point, subsequent carrying out the comparison for each pixel, an estimation of "1" would be allotted to the greater part of the pixels whose gray levels were lower than that of the fixed threshold, [and] "0" generally. But, if the threshold value limit esteem is less than the normal average of the shadow pixels, then a second image is required, where blobs having value"1" show the existence of shadows.

The earlier example explains a basic approach of segmentation. In industrial image processing application the essential thing is to extract the edges of objects and identifying their basic shapes. Acquiring boundaries from an image makes image analysis easier by radically minimizing the amount of data to be processed simultaneously it preserves valuable data referring to edges. Several filter for detection of edges have been suggested, for example Canny [5], Robert, Prewitt [6] and Sobel [7].

1.2.1 Implementations of Image Segmentation:

- Distinguishing objects from knowledge of appearance or dimensions such as shape and size .
- Object-based video compression (MPEG4) is used to classify the objects in a moving scene.
- Find cancer and other pathologies.
- Estimate tissue sizes.

- Computer-guided surgery.
- Machine Vision.
- Brake light identification.
- Traffic control systems.
- Find substances such as roads, greenery, housed in images captured with the help of satellite.
- Identification of different finger prints.
- Identification of dissimilar faces.
- Examining anatomical structure.
- Treatment Planning.
- Diagnosis.

1.3 Image De-noising Techniques

Removal of noise from an image is a main task in field of digital image processing such as a handle itself and in addition a part in different procedures. There are various methods and ways are exists to de-noise an image or a set of data. The good quality noise removal image is that in which noise is completely eliminated beyond what many would consider possible and in addition protect edges. Linear models and non-linear models are normally used for de-noising in a image. In general, linear models are applied. The constraint of linear noise removing models are, the models are not ready to save images of the image in an effective way such as edges, that are perceived as discontinuities in the image are spread out and the advantage of using is its speed of removing noise. Yet again, in comparison with the linear models non-direct models can deal much better with the extracted edges [8].

1.3.1 MEAN FILTER

Linear filters can be used to eliminate specific types of noise. In this regard specific filters, for example a Gaussian or Averaging filters are appropriate. Such as an average filter is used to remove grain noise in an image. Local changes due to the grain noise get minimized when each pixel is replaced by the number acquired after taking the average of all neighbourhood pixels. Usually in digital image processing, algorithms of linear filtering were used. The important and the uncomplicated of these algorithms is the Mean Filter as well-defined in [6]. Over every pixel in the image the mean filter that is a linear filter uses a mask.

This filter is a simple sliding-mask that replaces all pixels in the input image that fall under the window with the average value of each pixel lies in the mask. Normally window of this filter is square however it can be in any form. It is also known as average filter. The mean filter is not good in retaining boundaries of an image. It is defined as:

$$\text{Mean filter } (x_1 \ldots\ldots x_n) = - \sum_{i=1} x_i \quad (1.3.1)$$

For eliminating noise normally linear filters are applied.

1.3.2 MEDIAN FILTER

Like average or mean filter it is generally used for noise reduction in the image. Although, it's working in retaining valued parts in image is better than the average filter. It is a nonlinear digital filtering technique. The very initial step of pre-processing step is to find good results of getting on processing such as detection of edges in input image. In image processing, median filtering is really applied for the reason that under explicit environments, it protects edges together as eliminating noise. It works as a sliding-mask spatial filter, however it swaps the center value in the mask with the median of all the pixel values in the mask. The median for all the pixels of the input image is computed by initial arrangement of every adjacent neighbourhood pixel value into statistical way in addition to substituting the pixel being allocated with the pixel value which exists in the middle. The key point is that if the mask has an odd number of appearances, then it is requires to define median at that point, when all the entries in the window are settled numerically then it is middle value of the window. There is more than one possible median for even number of appearances. This filter is resilient. Median filters are extensively used in digital image processing as a smoothers and also in processing of digital signal in addition to processing of phase sequence. The main advantage of median filter against linear filters is that it may eradicate the effect of input noise using particular enormous magnitudes. Linear filters as compared to nonlinear filters are complex to such type of noise explicitly, the resulting output may be ruined severely by smooth by an insignificant portion of asymmetrical noise values [6]. "t" can be computed by taking the median of the input values corresponding to the instants coherent to t the output y:

$$y(t) = \text{median}((x(t\text{-}T/2),x(t\text{-}T_1\text{+}1),\ldots,x(t),\ldots,x(t\text{ +}T/2)) \quad (1.3.2)$$

Whereas t is used to define the size of median filter window, x is input image values and y is the corresponding output. Further the one-dimensional median filter is explained above, there are two-dimensional filters are also used in digital image processing. Generally digital images are

stored in form of two dimensional arrays of image components, or pixels for example sets of non-negative values B_{xy}ordered by two indexes

$$x = 1\ldots N_i \text{ (rows) and } y = 1\ldots N_j \text{ (column).}$$

where the components B_{xy} are scalar values, there are methods for processing color images, where every pixel is defined by number of values as every pixel has its red, green and blue values which is also used to determine the RGB value of pixel.

1.3.3 WEINER FILTER

This filter is used to supress noise which ruined the signal. It is influenced by quantifiable methodology. Normally filters are used to get desired frequency response. Weiner filter handles filtering from a diverse approach [10]. It is expected to have the knowledge of spectral characteristics of the noise along with new signal, while at the same time one finds LTI channel whose output would probably come close to the new signal. Such type of filters are explained below:

a. Hypothesis: with familiar spectral attributes signal in addition to additive noise are static linear casual procedures.

b. Condition: the filter should be physically attainable, for example causal, this prerequisite could be released, bringing about in a non-causal arrangement. Performance standards: least average-square error.

1.3.3.1 Wiener Filter Deconvolution

The Wiener filter is:

$$G(x,y) = \frac{H*(x,y)P_s(x,y)}{|H(x,y)|^2 P_s(x,y) + P_n(x,y)} \quad (1.3.3)$$

By dividing the above equation by P_s makes easy to describe its function:

$$\frac{H*(x,y)}{|H(x,y)|^2 + \frac{Pn(x,y)}{P_s(x,y)}} \quad (1.3.4)$$

Where,

H(x, y) = Degradation function

H*(x, y) = Complex conjugate of degradation function

P_n (x, y) = Power Spectral Density of Noise

P_s (x , y) = Power Spectral Density of un-degraded image

The term P_n / P_s may be taken as the inverse of the signal-to-noise ratio.

1.4 DIGITAL CAMERA IMAGE NOISE

The image noise in the images that are captured through digital camera is the arbitrary fluctuations of intensity or color data in images delivered by the sensor and hardware of a scanner or advance camera. Image noise could likewise begin in image particle and in the necessary shot noise of a perfect photon indicator [11]. Normally image noise is considered as an unwanted consequence of image taken. While such undesirable variations got to be known known as "sound" by similarity with undesirable noise they are indiscernible besides, for example indecisive. Following are the types of noise:-

- Gaussian Noise (Amplifier Noise)
- Speckle Noise
- Poisson Noise (Shot Noise)
- Salt-and-pepper Noise

1.4.1 Gaussian noise

The typical model of Gaussian noise is additive, amplifier, not dependent at every pixel and also not dependent of the signal brightness. In digital cameras having colored images where more intensification is utilized as a part of blue shading direct in comparison with the green or red channel, there is a possibility that blue color may have more noise. Gaussian noise is a noteworthy part of the noise of a film sensor, which is, level of noise is constant all over the dark regions of the image [12].

1.4.2 Salt-and-pepper noise

An image having dark pixels in high intensity areas and high intensity pixels in dark areas will have salt-and-pepper noise [12]. Salt-and-pepper noise may be originated by defective pixels, errors occurred due to analog to digital conversion, bit error rate in broadcasting, etc. It could be removed in huge portion by utilizing shady edge removal and by incorporating low intensity pixels/high intensity pixels all over the place.

1.4.3 Poisson noise

This type of electronic noise that occurs when the limited amount of elements that transmit energy, for example as electrons in an electrical circuit or photons in an photosensitive instrument this type of electronic noise is occurred which is slightly sufficient to provide intensification to measureable analytical variations in a dimension [12].

1.4.4 Speckle noise

Speckle noise is a grainy noise which intrinsically occurs in also damages the quality of the images captured by using SAR (active radar and synthetic aperture radar). This noise in ordinary radar comes from arbitrary variation in the arrival signal from an entity that is no greater than a particular image-processing component. Speckle noise rises the average grey level of a limited region. This noise in SAR is normally very severe, producing complications for image analysis. The coherent processing of backscattered signals from several scattered goals produces this types of noise. In SAR oceanography [13], such speckle noise is originated by signals from basic distributes, the gravity-capillary waves as well as establishes as a support image, below the image of the sea waves.

1.5 Histogram

The range of grey levels in the histogram is a discrete function $n_k = r_k$ of a digital image varies from 0 to L-1. Here, n_k represents the number of pixel in the image which has that grey level and r_k represents the kth gray level. When intensity value of every pixel is divided by the entire number of pixels in an image usually represented by "n", histogram gets normalized and it is called normalized histogram. As a result, it can be shown mathematically as, p (r_k) = n_k/n, where n is the total number of pixels and k=0,1,. . ., L-1. It is safe to say that function p (r_k) gives an approximation of possibility of r_k occurrence. Normalized histogram is always equivalent to one when it's all components added together, since it is basically probability. A number of spatial domain processing techniques are based on histogram [14]. Not only do they provide useful image statistics, they also help in reducing the size of digital image as well as in detection of edges. It is normally believed that histograms are effective because implementation, both in hardware and software, is quite easy. Here are a few things about my images' histograms. For an image, which is absolutely noise free, two clear spikes for i=100 and i=50 can be seen. However, for an image with low noise value, there have been found two peaks, centering on the same values as for a noise free image. There is only one peak for image having a higher noise content. Single peak suggests the overlapping or merging of object and background grey levels. The input image SNR can be defined in terms of: background pixels of an object and foreground pixels and a depression of additive white gaussian noise[15].

$$S/N = \frac{|\mu_0 - \mu_0|}{\sigma} \qquad (1.5.1)$$

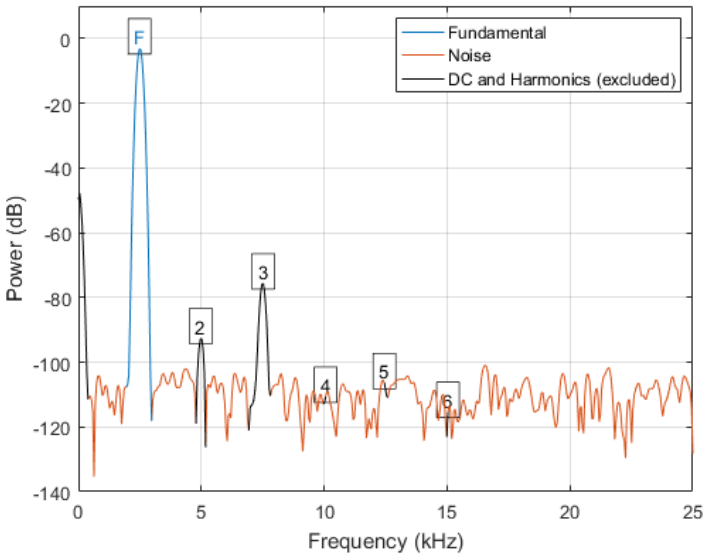

Figure 1.1: Signal to noise ratio of a signal

1.5.1 THRESHOLDING (Image Segmentation)

It is easiest technique to segment an image. For the purpose of thresholding, a minimum threshold is defined. Any pixels with values greater than that threshold, would be considered to be belonging to the object. This technique is useful under the assumption that the object is brighter than the background. This technique is called “Threshold Above”. There is another thresholding technique that is the exact opposite of the previous one. It is called “Threshold Below”. Two other techniques are “Threshold Inside” and “Threshold Outside”. In both of these techniques, two threshold values are defined. However, in the former technique, pixels having values between those threshold points, are the object pixels, whereas in the later, those lying outside the range, are segmented as the object pixels. Typically, the value 1 is assigned to object pixels whereas the value 0 is assigned to the background pixels. Then, using the segmentation and new values, a binary image is created where object is colored white while the background is black [16].

Thresholding provides an easy solution to understand the foreground and background parts of the image in terms of segmentation [17]. It can be easily observed a definite valley between the two points. Thresholding of gray level image can be defined in a following manner.

If the intensity value of pixel “p” of an image is less than the thresholding value then pixel “p” belongs to foreground of an image otherwise it is a pixel of background.

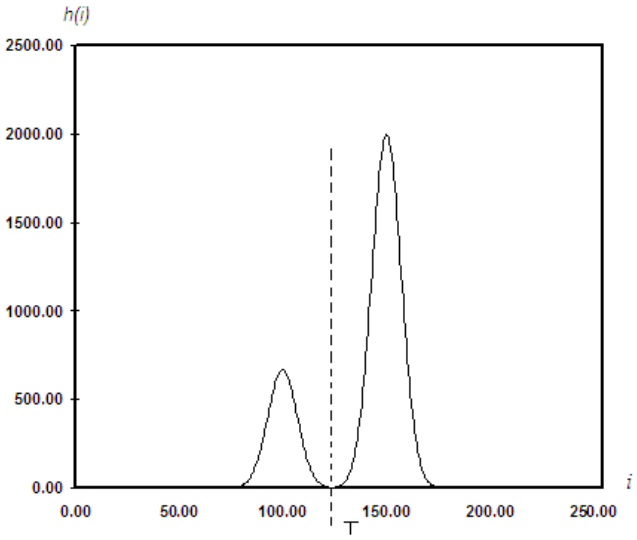

Figure 1.2: Thresholding of an Image

1.6 Methods of Edge Detection

Edge detection can be done in multiple ways. However, these can be categorized in two broader categories [18]:

a. Gradient: This method employs first derivatives of image for finding maximum and minimum values.

b. Laplacian: It finds edges by finding out the zero crossings in the second derivative. Calculation of the derivative highlights the location of the edge. It is in one dimensional ramp shape.

A signal is showing in figure 1.3with an edge that represents transition in intensity levels.

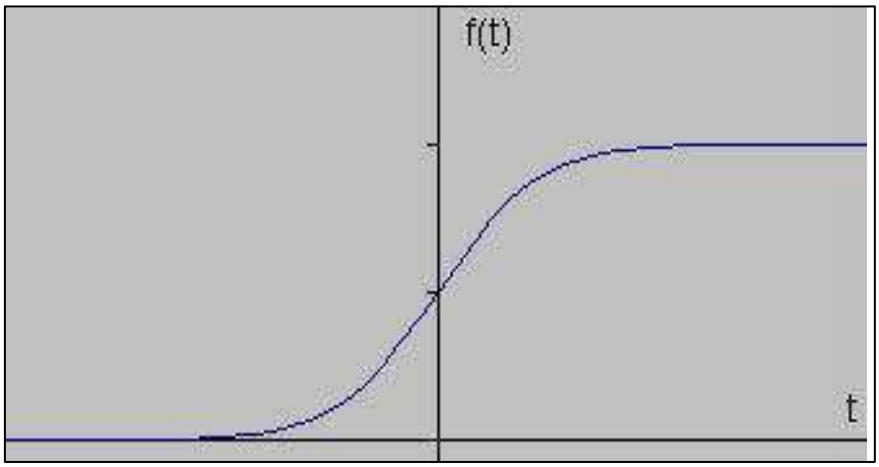

Figure 1.3: Signal Intensity Graph

If it is desired to observe the change occurs in one direction of the above signal then take its first derivative in one dimension with respect to "t" as shown below:

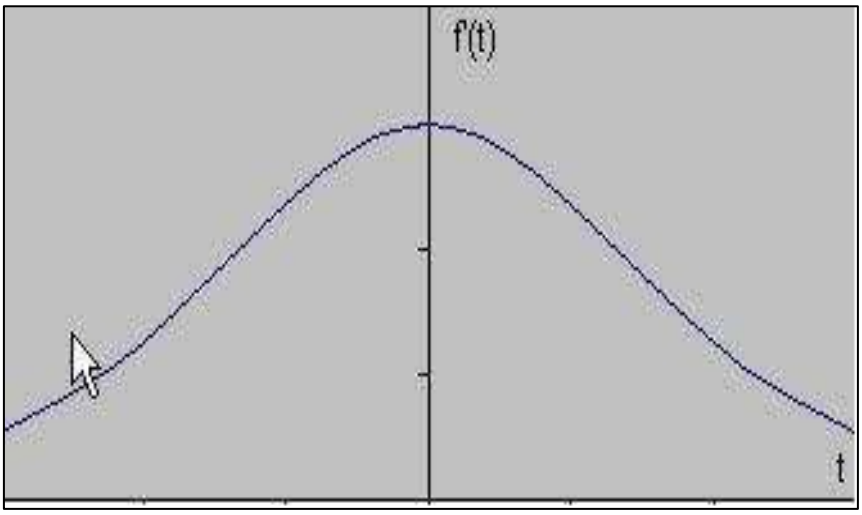

Figure 1.4: Gradient of Signal

After getting the first derivative of signal, it is found that maximum is positioned at the middle of the image. This edge location method is a mixture of "gradient filter" and Sobel method. Edge is identified only if the gradient value is greater than the threshold. An edge would have greater pixel intensity value compared to its surroundings. Therefore, setting a threshold is crucial to edge detection. Gradient values of each and every pixel would be compared to threshold, and if he value exceeded that threshold, edge would be declared. The second derivative must be at zero when first derivative is at maximum. Therefore, using this math rule, can also help us locating the edge[19]. It provides an alternative method to find the edge that is, finding the zero crossings. The above explained method is the Laplacian technique.

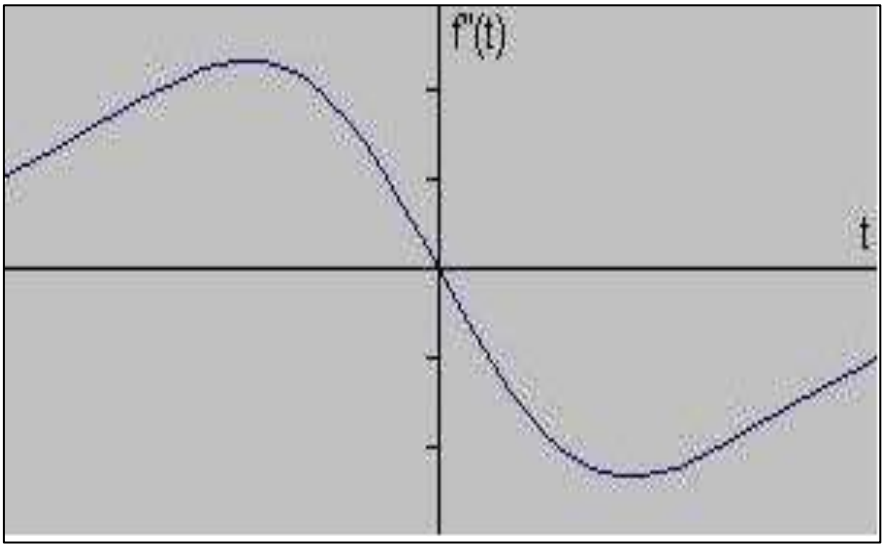

Figure 1.5: Second Derivative of the Signal

1.6.1 SOBEL OPERATOR

This operator usually implements in edge detection algorithms. They are used in many applications. To detect the abnormalities in retinal blood vessels sobel detector was used [20]. The edges of vehicles are detected with the help of sobel filter to implement a vehicle license plate detection system [21]. The sobel edge detector is used as template for multi-scale edge detectors [22]. It finds an estimated value of gradient image intensity function. At each point in the digital image, the output of the sobel operator is an equivalent gradient vector or norm of this vector. It performs its calculations by convolving the image with a small, separable and integer-valued filter, in both horizontal and vertical directions. This is what makes it comparatively inexpensive and cheap. One drawback of this operator is the crudeness of the gradient value it generates, especially in images with high frequency transitions.

In simpler terms, working of a Sobel operator [23] can be explained as: first, computation of gradient of image intensity to give a rough idea as to how the image transitions from pixel to pixel. Second, predicting the likelihood of presence of edge and also its orientation, depending upon the transitions and variations. Magnitude calculation has an edge over Sobel operator owing to its reliability.

In simpler terms, working of a Sobel operator can be explained as: first, computation of gradient of image intensity to give a rough idea as to how the image transitions from pixel to pixel. Second, predicting the likelihood of presence of edge and also its orientation, depending upon the transitions and variations. Magnitude calculation has an edge over Sobel operator owing to its reliability. It does simple convolution to create magnitudes [24]. For a group of pixels 'p', applying convolution k, mathematically we can express it as follows:

N(x,y) = (image segmentation using hough transform)

Therefore, Sobel operator uses two convolution kernels. One for detection of contrasts vertically (G_y) and other for doing the same in horizontal direction (G_x).

G_x =

-1	0	1
-2	0	1
-1	0	1

G_y =

-1	-2	-1
0	0	0
1	2	1

Figure 1.6: Mask of Sobel Edge Detector

The above data may be characterised as a gradient vector. The changes happening in x and y directions in an image can be calculated with the help of G_x and G_y which are horizontal (x-axis) and vertical (y-axis) components of vector. Therefore we have gradient magnitude and direction:

$$G = \begin{bmatrix} G_x \\ G_y \end{bmatrix} \quad \text{(1.6.1 image segmentation hough tranform)}$$

$$|G| = \sqrt{{G_x}^2 + {G_y}^2} \quad \text{(1.6.2 image segmentation hough tranform)}$$

$$\vartheta = tan^{-1}\left(\frac{G_y}{G_x}\right) \quad \text{(1.6.3 image segmentation Hough tranform)}$$

Where g is the gradient vector, g is the gradient magnitude and θ is the gradient direction.

1.6.2 CROSS OPERATOR of ROBERT

It executes 2D gradient dimensions on a digital image. This operator consists of 2 x2 convolution kernels. They have an angle difference of 90 degree. They respond with a maximum for edges running at 45 degrees [25].

$G_x =$

1	0
0	-1

$G_y =$

0	1
-1	0

Figure 1.7: Roberts Cross Operator

An input image can be subjected to the operator which in turn produce separate measurements for gradient component [26]. In order to detect the absolute magnitude of the gradient at every point and the direction of that gradient, all these 224 may be joined together.

Generally the equation 2.6 is used to calculate gradient magnitude:

$$G(x,y) = \sqrt{{G_x}^2 + {G_y}^2} \quad (1.6.4)$$

While an estimated magnitude is given by:

$$|G| = |G_x| + |G_y| \quad (1.6.5)$$

Which takes less computation time.

To find the edge's angle of direction equation 2.8 is used:

$$\vartheta(x,y) = \arctan\left(\frac{G_y(x,y)}{G_x(x,y)}\right) \quad (1.6.8)$$

1.6.3 PREWITT'S OPERATOR

It is quite similar to Sobel operator. It detects horizontal and vertical edges**.** If "B" is the input image, G_x is the image consisting of vertical derivatives of B and $G_y$is the image comprising of horizontal derivatives of B which are calculated as [27]:

$$G_x = \begin{bmatrix} -1 & 0 & +1 \\ -1 & 0 & +1 \\ -1 & 0 & +1 \end{bmatrix} \quad G_y = \begin{bmatrix} -1 & -1 & -1 \\ 0 & 0 & 0 \\ +1 & +1 & +1 \end{bmatrix}$$

Figure 1.8: Prewitt Edge Detector

Then perform convolution of G_x and G_y with B. These filters calculate the gradient with smoothing since the Prewitt filters may be fragmented as the products of a mean and a differentiation filter. Thus, it is also known as separable filter. Such as, G_x may be define as:

$$\begin{bmatrix} -1 & 0 & +1 \\ -1 & 0 & +1 \\ -1 & 0 & +1 \end{bmatrix} = \begin{bmatrix} 1 \\ 1 \\ 1 \end{bmatrix} [-1 \quad 0 \quad 1]$$

In right direction the x-coordinate is increasing and y-coordinate is increasing towards downward. The subsequent gradient estimations can be merged to find the magnitude of gradient at each point in the image, using this formula:

$$|G| = \sqrt{{G_x}^2 + {G_y}^2} \tag{1.6.9}$$

By utilizing this data, the direction of gradient can also be calculated:

$$\vartheta = atan2(G_y, G_x) \tag{1.6.10}$$

Whereas ϑ is a vertical edge direction which, if it is equal 0 then it will get darker on the right side.

1.6.4 LAPLACIAN OF GAUSSIAN

In a second spatial derivative of a digital image, the Laplacian is a 2-D isotropic magnitude. The quick variation in intensity of image is usually indicated by Laplacian and can be used for edge detection [28]. Any image having an approximation of Smoothing Gaussian filter solved by the Laplacian. Only a single image normally is as output by operator.

Image having pixel intensity I(x,y), its Laplacian L(x,y) is given as:

$$I(x,y) = \frac{\partial^2 I}{\partial x^2} + \frac{\partial^2 I}{\partial y^2} \tag{1.6.11}$$

As discrete pixels are used to represent the input image, approximation of second derivatives in Laplacian can be achieved by finding discrete convolution kernel. Figure 1.9 shows some commonly used small kernels.

$$\begin{bmatrix} 0 & 1 & 0 \\ 1 & -4 & 1 \\ 0 & 1 & 0 \end{bmatrix} \begin{bmatrix} 1 & 1 & 1 \\ 1 & -8 & 1 \\ 0 & 1 & 0 \end{bmatrix} \begin{bmatrix} -1 & 2 & -1 \\ 2 & -4 & 2 \\ -1 & 2 & -1 \end{bmatrix}$$

Figure 1.9: Laplacian Edge Detector

These derivatives (second) are as kernels approximation are sensitive to small noise measurement. Before application of Laplacian, image is get Gaussian Smoothed to cope up with it. Earlier to differentiation step, this step lessens the high frequency noise constituents.

As the convolution operation is associative, Laplacian filter can also be convolved by Gaussian smoothing filter first, then result of this combined convolution filter is used to attain the necessary output. Continuing in this manner is beneficial in two means:

It requires lesser arithmetic operations as Laplacian kernels and Gaussian are very much small than image. Only a single convolution is to be calculated on image because of advance calculation of The LoG (`Laplacian of Gaussian') kernel.

The 2-D Gaussian standard deviation σ and LoG function concentrated on zero and with has the form:

$$\text{Log}(x,y) = -\frac{1}{\pi\sigma^4}\left[1 - \frac{x^2+y^2}{2\sigma^2}\right] e^{-\frac{x^2+y^2}{2\sigma^2}} \qquad (1.6.12)[24]$$

and is shown in Figure 1.10.

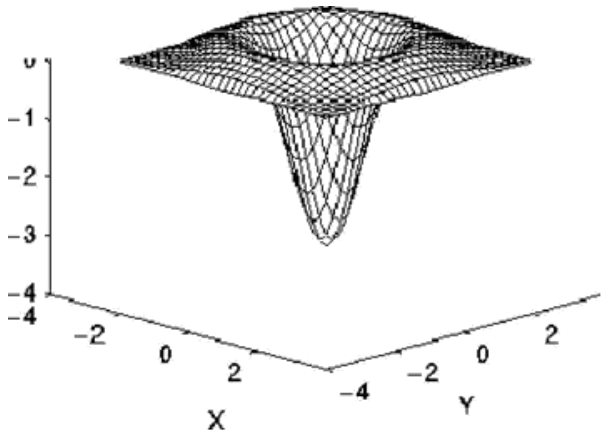

Figure 1.10: Gaussian Surface

0	1	1	2	2	2	1	1	0
1	2	4	5	5	5	4	2	1
1	4	5	3	0	3	5	4	1
2	5	3	-12	-24	-12	3	5	2
2	5	0	-24	-40	-24	0	5	2
2	5	3	-12	-24	-12	3	5	2
1	4	5	3	0	3	5	4	1
1	2	4	5	5	5	4	2	1
0	1	1	2	2	2	1	1	0

Figure 1.11: Digital Approximation to LOG function

LoG kernel turn out to be the same as the unpretentious Laplacian kernels because the Gaussian is ended gradually narrow, shown in Figure. When Gaussian is less than 0.5 pixels on a digital grid, it has no result. The unpretentious Laplacian on discrete grid may be perceived as a restraining case of the LoG for tapered Gaussians.

1.6.5 CANNY'S EDGE DETECTOR

Many researchers used this edge detection technique to achieve different goals. For image steganography, canny edge detectors are used to detect the edges of an image and then the message is covered in edges by implementing former component adaptation method [29]. To extract the building vertical edges based on high resolution image canny operator has been used [30].The Canny operator was used in the edge detection of fabric sample with defects. The canny edge detector first uniforms the image to wipe out the gradient to point out the peak regions with high spatial subordinates. The calculation then tracks along these regions and smothers any pixel that is not at the most highest point (non-greatest concealment). The slope array is presently additionally minimize the left over pixels that have not been removed. Two threshold values are used in hysteresis and if the point is below the first threshold value, it is fixed to zero or non-edge. On the other side if the point lies above the second threshold value, it is set to one. If the point lies in between the two given edges it then it is set to zero except it there is any solution exists from pixel to a pixel using a slope beyond another edge.

1.7 HOUGH TRANSFORM

In Hough transform it is considered that point lie on the edge of a shape are connected [31]. Despite of the local study way where known number of points (i.e. n) of an image are taking into account. Assume that it is required to compute the subset of such points which exist on edges of straight line. One practicable method is to detect every line calculated for every coordinate then at that time obtain all coordinates which are near to precise straight lines [32]. For the comparison of each point of entire lines it first computes n (n-1)/2 ~ n^2 lines then execute (n) (n (n-1)) ~ n^3 which is basic issue with the implementation of this method. The computations of this method is very limiting in everything except in most the minor applications. With the help of the Hough

transform, characteristics of different shapes in the image can be examined theoretically. In implementation it is generally used for detection of circles and straight lines [33]. The difficulty level of computations of this method grows promptly with further intricate figures. Consider some pixel values in an image which are maybe the outcome of an edge finding procedure or points lie on the border of a binary splotch. To find the points that makes a line.

Suppose a coordinate in the image which is located at (x_i, y_i). Equation of a straight line in standard form is:

$$y = ax + b \tag{1.7.1}$$

Infinite number of lines are going through this point, however all these lines fulfil the constraints.

$$y_i = ax_i + b \tag{1.7.2}$$

The above equation can be rewrite if "a" and "b" will vary in following way:

$$b = -x_i a + yi, \tag{1.7.3}$$

Then show the changes of a and b on graph.

Votes can be added in ab-space from every coordinate in xy-plane with the condition that the parameter accumulator array is distributed into a number of distinct accumulator blocks. The equation of co-linearity of points in xy-plane indicates highest points in ab-plane.

When the line is vertical that cosα approaches to infinity as well as the parameter space is infinite, then to define equation by using equation y = ax+b is still a big problem (it needs a very large memory to store parameter space)

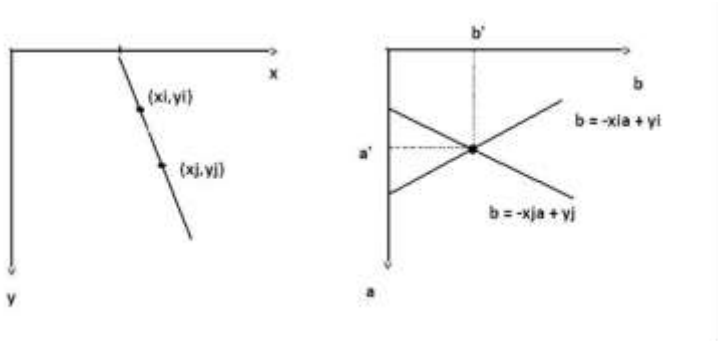

Figure 1.12: XY-Plane and Parameter Space

Another method to represent line is given by:

$$\rho = x\cos\vartheta + y\sin\vartheta \qquad (1.7.4)[28]$$

Where ρ is the distance between points of line and origin and θ is the angle between x-axis and the line perpendicular to origin. So, parameter accumulator array is now in theta and radius whereas theta ranges from 0 to 2π and radius is bounded by the dimension of the image.

Highest points in the accumulator array specify the equations of important straight lines as it was explained previously

1.7.1 ACCUMULATOR

In the digital image, detection of prominent lines may be expressed as detecting every one of the areas in parameter accumulator array where huge number of lines cross each other. It is primary objective of Hough Transform. With a specific end goal to calculate the Hough Transform, should select on a digital introduction of the steady parameter gatherer cluster by choosing a proper stride estimate for the k and d axes [34]. When stride evaluation is chosen for the directions, the space could be presented logically by an array. Accumulator array if formed when lines intersects. Accumulator array paints every parameter space line as well as the cells through which it experiences are expanded so that in the end each cell totals number of lines that bisect at each cell as shown in figure 1.13.

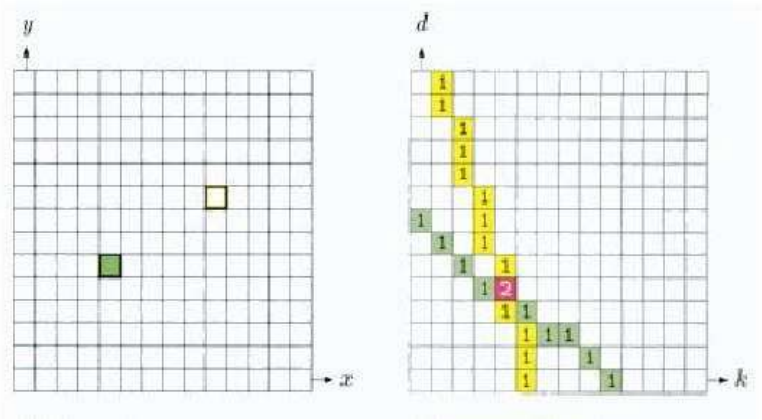

Figure 1.13: Space of Image and Parameter

1.7.2 BASIC ALGORITHMS

- The RGB digital image is converted into binary image and then find the edges of the binary image by using any edge detection technique before implementing hough transform [35].
- To reduce the computation load hough transform uses gradient information.
- Values of ρ and θ-plane become limited.
- It generates an accumulator array X (ρ, ϑ) in which initially all values are set to zero.
- For every edge point (x_n, y_n) in the image, it uses gradient direction to find the value ϑ. After this it computes the value of ρ from the equation and then it increment X (ρ, ϑ).
- It searches the maximum value of X (ρ, ϑ) for every cell in X (ρ, ϑ) and calculate equation of line.
- Also it observes the connection (principle of continuity) between pixels in a selected cell. The principle of continuity can be observed by computing the distance between pixels that are not directly connected recognised for the duration of crossing of the set of pixels relating to a identified accumulator cell.

If the computed distance between that point and its nearest neighbour go beyond a specific threshold then a discontinuity at any point is irrelevant.

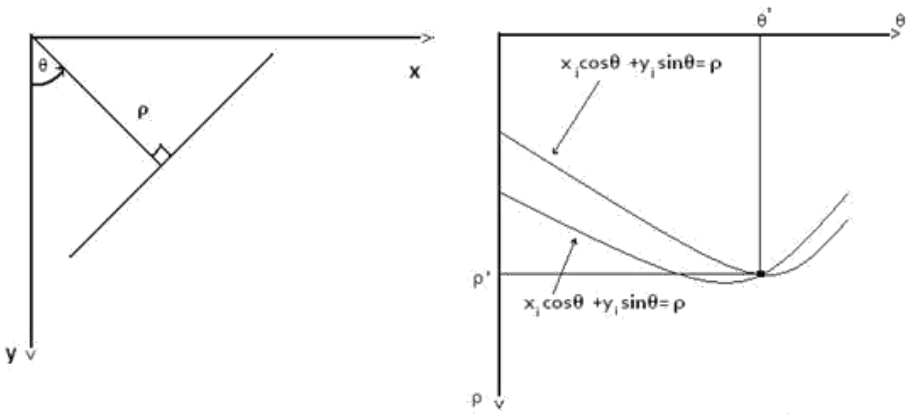

Figure 1.14: Parameterization of Line in the XY-Space and Sinusoidal curve in the ρθ-Space

1.7.3 CIRCULAR HOUGH TRANSFORM

The Circular Hough transform can be used to extract the features of circle in any kind of image though the difficulty of the conversion rises with the number of feature required to define the contour. Circular Hough transform (CHT) is explained below [36].

1.7.4 PARAMETEER REPRESENTATION

The exchange of each point in the 2D plane to the parameter space is a function Hough Transform. The parameter accumulator array is well-defined by giving the parameters need to be find of the shape of interest.

The circle is easily be presented in parameter accumulator array in contrast to the line, as the features of the circle can be simply transform to the parameter space.

The equation of the circle is:

$$r^2 = (x-a)^2+(y-b)^2 \tag{1.7.5}$$

where a and b are the pair of points of the centre of the circle in the direction x and y respectively and r is the radius of the circle. a , b and r are three parameters need to define the circle.

The pair of points of circle can be calculated by using this formula:

$$x = a + r\cos\theta$$
$$y = b + r\sin\vartheta$$

Thus the parameter space of circle is 3-D while the line has two parameters for example x and y so it belongs to 2-D. The difficulty of Hough transform increases by increasing the number

of parameters required to define the shape as the dimension of the parameter space increases. Parameters of uncomplicated shapes link to 2-D or as a maximum 3-D .So as to ease the parametric illustration of the circle, the value of radius can be set constant or known radii with limited number.

1.7.5 ACCUMULATOR

By using Circular Hough Transform the procedure of detecting the circle in the image is explained. In the first steps edges of all objects in the image needs to be detected with the help of any edge detection technique. Canny, Robert's cross operator or Prewitt all these edge detectors can be used to find edges of the objects. Sobel edge detection technique is used in this project. A circle is drawn at every edge provided the pair of points of centre with the required radius. Circles are drawn in the parameter space, for example value of "a" lies on the x-axis and value of "b" lies on y-axis and the radii lies on z-axis [37]. At the directions which has a place with the parameter of the drawn circle. Due to the same size of accumulator array and parameter space, the value in the accumulator is increment by one. Like this, it clears over vitality it draws circle with required radius on input image and then take values from accumulator array one by one. Return to accumulator which would currently consist numbers resembling to the shape of circles going over the distinct coordinate as soon as each edge point besides each required radius is utilized [38]. Therefore the maximum number resemble to the circle of the circle in the input image.

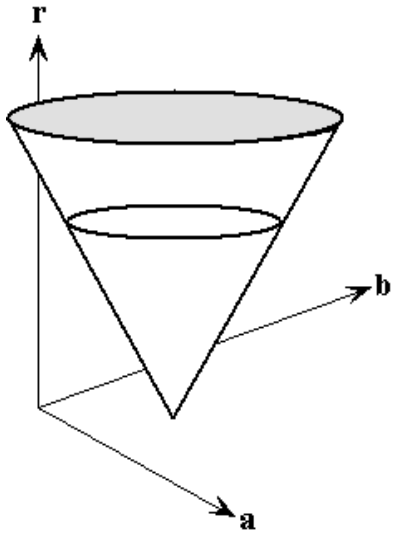

Figure 1.15: CHT Parameter Space

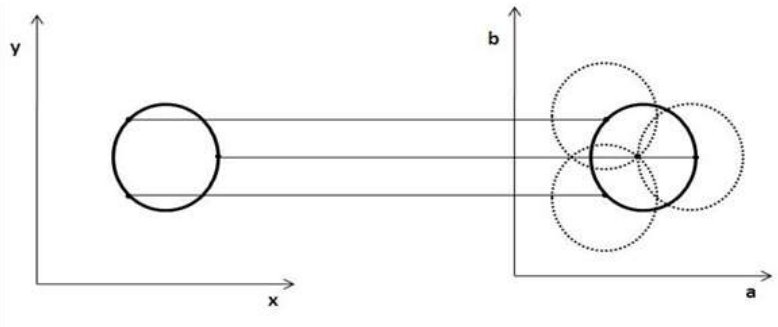

Figure 1.16: A CHT from the XY-Space to the Parameter Space

1.7.6 ADVANTAGES

One essential differentiation between the Hough Transform and diverse methodologies is hesitant of the past to noise in the info image and its strength towards crevices in the breaking point line [39]. There is a comparison shown in Figures 1 and 2 of a plain straight line with a spotted one. Such as it could be observed there is practically no distinctions in the outcomes.

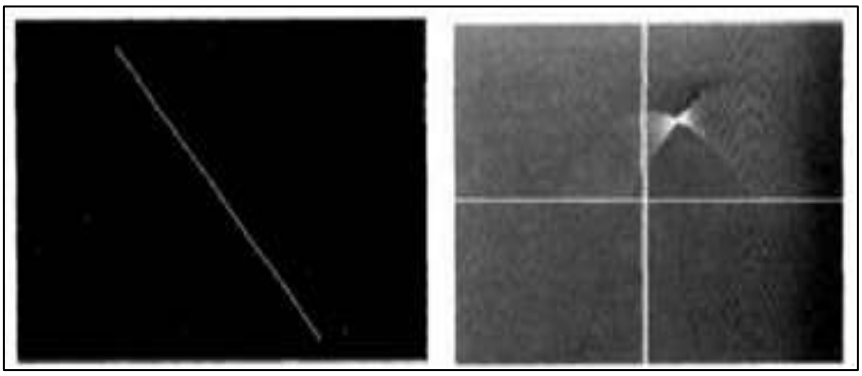

Figure 1.17: Straight line and its HT. This figure shows a straight line and its Hough Transform.

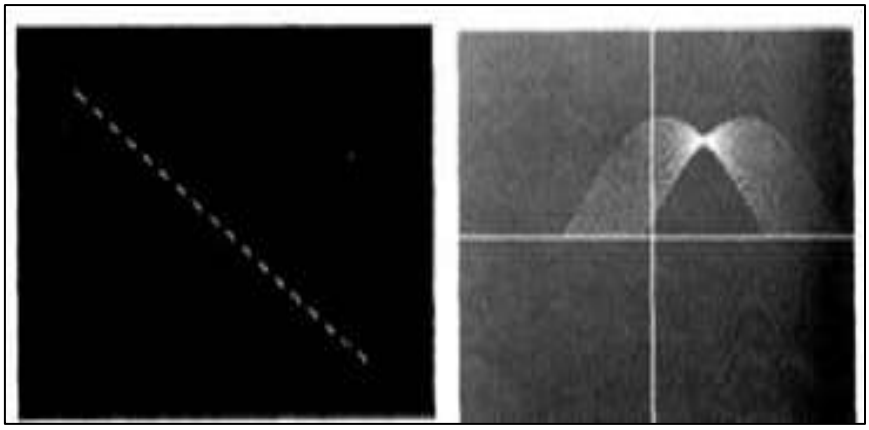

Figure 1.18: Straight Dashed line and its HT. A straight dashed line and its hough transform has shown in this figure.

CHAPTER 2: IMPLEMENTATION

2.1 Hardware

The hardware for this machine vision system consists of a camera (DSLR), a transparent surface, a tripod stand and a PC. The DSLR camera used in order to capture images of Connecting-rod has its details such as 5184x3456 Pixels, 14 bit depth JPEG/JPG file format and manual brightness adjustment with brightness compensation.

It is required to install illumination system accurately in order to acquire images. The necessity is to extract edges of the Connecting-Rod. Due to front lighting, it is observed that shadow appears in the acquired image and as a result when image is processed it detects incorrect edges. So the brightness of the DSLR camera is adjusted manually to get maximum illumination in order to get rid out of this problem. Still a little crescent is left in the image which is further resolved with the aid of software. The distance between the DSLR camera and the Connecting-rod is fixed i.e 75cm.

There is an inverse relation between distance from where image is captured and number of pixels in an image. The relation between distance or the height of the camera and number of pixels are shown in figure 2.1.

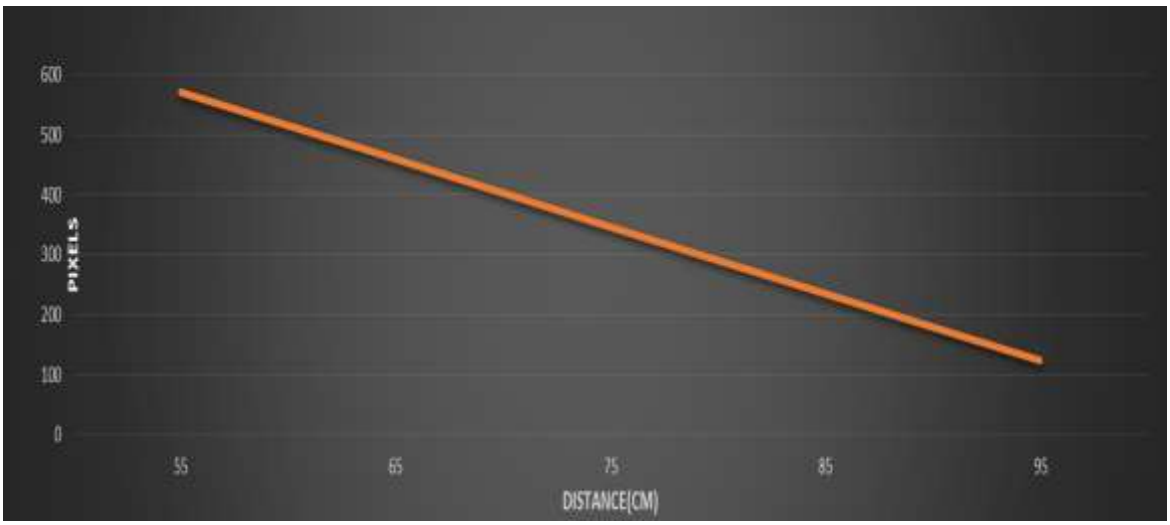

Figure 2.1: Relationship between Distance and Number of Pixels. This figure shows how number of pixels are varying with distance.

2.2 Software

Softwares like MATLAB, OpenCV, MV Impact, labVIEW will give various digital images preparing strategies utilized for getting required data from acquired digital images.

- Here Matlab is used for image processing and analysing after capturing images.

- The quality of the Connecting-rod is showed according to the necessary quality parameter that is K as examined by the Matlab.

In MATLAB software, there is an IAT (Image acquisition toolbox) which is used to acquire images [40]. This toolbox have various functions which enhance the competence of MATLAB also it allows different operations on images after acquiring them by using various image acquisition tools in order to achieve desired results[41]. From professional-grade frame grabbers to USB-based cameras there are number of devices that are used for image acquisition [42]. IAT identifies compatible video acquisition devices as well as image acquisition devices [43]. The main benefit of using this toolbox is that it allows frames acquisition at high speed at which the camera and the system support its image acquisition speed [43]. A digital image is stored in form of a matrix which is 2 dimensional for example f(x, y), where x and y are the locations of pixels, and the value of "f" at any pair of (x, y) is intensity or gray level of the pixel at that location [44]. The values of x, y and "f" in a digital image are discrete and finite.

Each component which has a finite amplitude at coordinate (x,y) is termed a pixel[45]. Image resolution can get by multiplying the number of pixel rows with a number of pixel columns in the matrix [46]. Size of the image depends on Camera specifications. The image can be resized if its size image is too large[47] e.g: there is an image of size 1280x600, it can resized into a smaller size e.g 600x480 using the MATLAB built-in command of imresize. Image name and size at which image is to be resized should be defined.

CHAPTER 3: METHODOLGY

There are two main parameters of connecting-rod that needs to be measured perfectly, where the connecting-rod links the piston to the crankshaft to make a simple mechanism which changes the to and fro motion into rotary motion. It is not viable to insert the crankshaft into the typical sized bearing if the diameter of connecting-rod is more or not accurate. Therefore the diameter of rod is ensured using machine vision before inset of bearing in shaft [48]. In this, the requirement is to detect the large bore and small bore diameters located in two places of each connecting-rod with the below classifications:

i) OK component.

ii) Not OK component – over size.

iii) Not OK component – under size.

The components that are under sized go as scrap whereas the oversized components are send back to modification. The machinist picks part from the screen for the given part. The piece is positioned on the holder. Then camera takes images of the piece and sends them to the computer. Next, Matlab is used for processing of images [49] and the result is showed on the screen.

Figure 3.1 illustrates the methodology followed by proposed quality inspection system for connecting-rod.

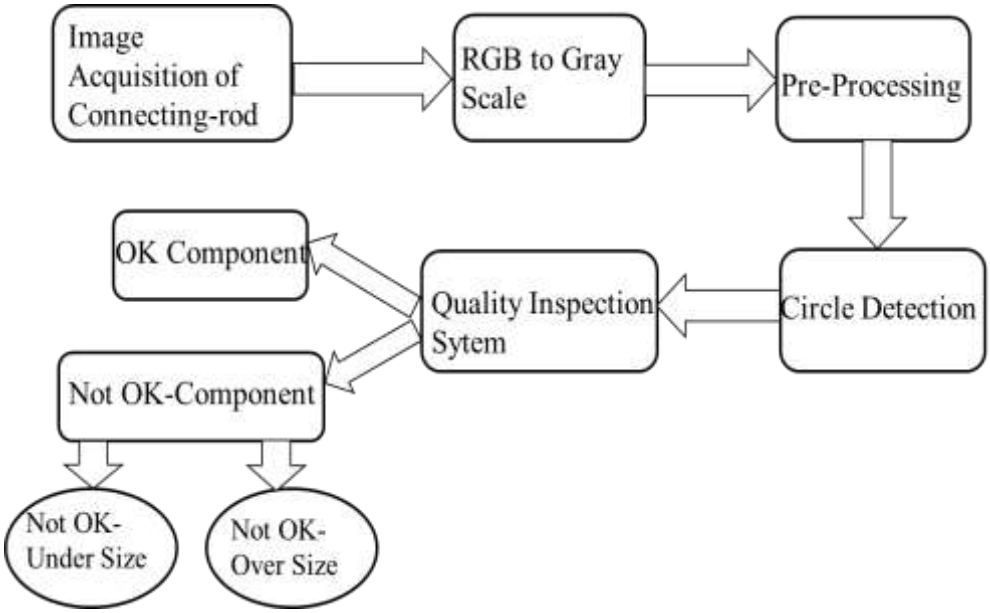

Figure 3.1: Block Diagram of Connecting- rods defect detection and classification. This figure shows

3.1 Pre-Processing

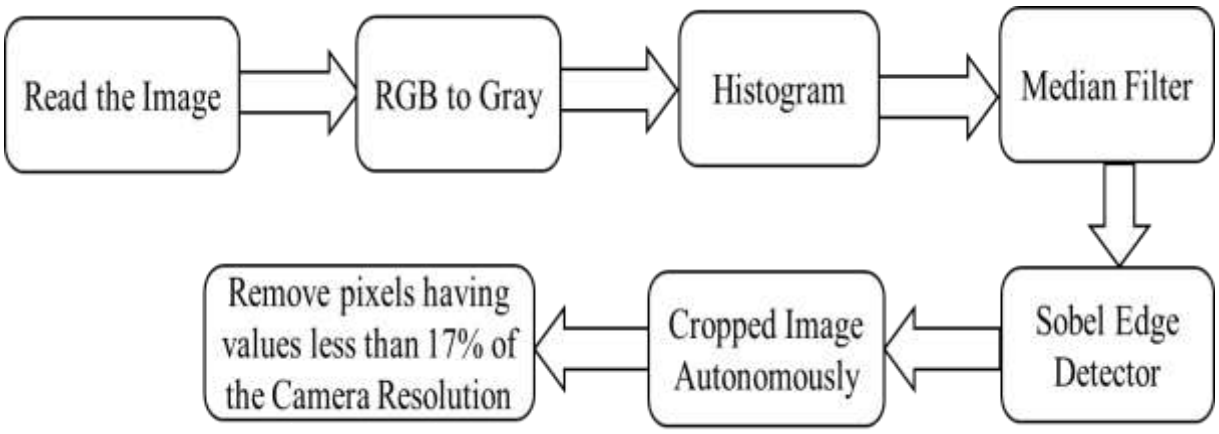

Figure 3.2: The Flow of Image Processing and Analysing. Steps of pre-processing followed by algorithm are shown in this figure.

- Once image is captured, the first step is to read it.
- To decrease computational intricacy the RGB image converts into Gray scale.
- Draw the histogram of the image. To get the information about intensities of pixels, Histogram is drawn.
- To eliminate noise from image Median filter is used.
- Sobel Edge detector is used to identify edges in the image.
- Therefore algorithms for detecting edges are generally used to gather significant information of edge pixels.
- Original image is cropped to extract the meaningful part of image for further processing.
- To remove crescent from the images an “area opening” function is used which removes all linked components that have less than P pixels from a binary image which gives another binary image.

3.2 Method I: Circular Hough Transform

To identify lines in an image, Hough Transform is normally used. “hough” function is used to implement the hough transform [50].

Syntax:

[H, T, R] = hough(B, ntheta ,nrho,peaks)

Inputs:

B is the resultant image that is acquired after applying edge operator on input image.

The intervals between Hough Transform bins along the "theta" axis is defined by ntheta and nrho defines its bins spacing along the "rh"o axis. Houghpeaks returns the peaks in the form of matrix that has the x and y locations of bins so as to utilize in detecting lines. The lines returned by "hough" are a structure array whose span matches with the number of combined line segments searched.

Outputs:

prho-by-ptheta is the resultant matrix named as H of the hough transform .

Whereas,

$$\text{prho} = 2*\text{ceil}(\text{norm}(\text{size}(I))/\text{qrhon}) - 1,$$
$$\text{ptheta} = 2*\text{ceil}(90/\text{qthetan})$$

All columns and rows of matrix of H has their corresponding ptheta and prho vectors. Every collinear line in the xy-plane meets at one point in ρθ-plane.

To detect Hough peaks first search the Hough Transform cell which has a maximum value then save its position [51]. Then fixed the values of cells to "0" in the instant vicinity of the highest attained already. The process is repeated till desired number of peaks has been located, or till defined threshold has been hitted. "houghpeaks" uses the below mentioned method to detect peaks.

Syntax:

[rw, cl, Hn] = houghpeaks(H, numpeaks)

Inputs:

"houghpeaks" identify the peaks in the hough transform matrix H. Generally highest number of peak position is defined by "numpeaks". If the value of H is less than the set threshold at that time it must not remain supposed as a peak. "nhood" can also be given as input to Houghpeaks which is a vector having two elements for example coordinates of rows and columns of peaks, illustrates the dimension of eliminating region. Once the peak is detected the region around every peak is suppressed.

Output:

"rw" and "cl" are the rows and columns having xy-values of the identified peaks. "hn" is the output of Houghpeaks which returns hough transform with peak region eliminated.

As soon as Hough Transform detects the set of peaks, it stays to be fixed. The initial step for all peaks is to locate the area of all nonzero pixels in the digital image that added to particular peak.

[rwn , clmn] = houghpixels(I,theta,rho,rbin,cbin)

To draw specific bins for Hough Transform "houghpixels" calculates coordinates of row-column (rwn, clmn) for pixels having values other than zero in an image. In the hough tansform matrix "rbin" and "cbin" are scalar quantities specifying the position of row-column bin. The second and third obtainable arguments from the hough function is ρ and θ. The pixel linked with the positions should be assembles in shape of a line segment which are detected by implementing "houghpixels". "houghlines" uses the following procedure [52]:

- Rotate the image at 90° so that every pixel lie along a y-axis.
- Find the position of pixel from the rotated image.
- To find spaces "diff" function has been used. Disregard little spaces; this has impact of consolidating neighbouring line portion.

Syntax:

L = houghlines(I, TH, RH, RX,CY , 'FILLGAP' , 'MinLength')

To extricate line segments in the image I connected with specific Hough Transform bins, "houghlines" is used. The output given by the "houghlines" consists of ρ and θ which are vectors. Two number vectors of Hough Tansform bins are used in detection of line segment which are "RX" and "CY", row and column vectors respectively. When "houghlines" finds two line segments connected with the same Hough Transform receptacle that are isolated by not as much as fillgap pixel then it combines these two lines into one line segment. Combined line segments are not as much as minlength pixels along are disposed of.

3.2.1 FOR CIRCLE DETECTION

"houghcircle" is used to identify various circles in an image with the help of hough transform. The image has circles whose centers might be lie inside the image or outside of the image [53].

Syntax:

centers = imfindcircles(img, radius);

or

centers = houghcircle(img, [MINR MAXR], ratio);

Inputs:

img: It is an input image. It can be gray image or a colored image.

MINR: minimum radius set for circle needs to be detect. Units of radius are in pixels

MAXR: maximum radius set for circle which units are also measured in pixels.

Ratio: minimum number of edge pixels that are detected from the circle perimeter. Normally ratio is set between 0 and 1.

Output:

The output of houghcircle gives values of radius and centers for each detected circle in an image. where (cx cy), R, and c are the center coordinate, radius, and pixel count, respectively. Following are the steps which are followed by output.

In its first phase it checks input parameters.

- Delta is equal to 12 only if number of inputs is 4 as every component of circle center and radius can be vary 3-5 pixels approximately.
- When there are four input parameters then the ratio is equal to 0.4 that is ¼ of the perimeter of circle and delta is equal to 12 in that case.
- The program shows an error that minimum 3 input arguments are required when the number of input is not 5.
- Convert the RGB image into Gray scale image.
- Generate an array which must be three dimensional Hough array. The first two dimensions represent the direction of the circle center and the third shows its radius.
- Sobel opertaor is used to identify edge pixels. To adjust between the execution and identification quality set the lower and upper limits.
- For a pixel lies on edge perimeter of the circle, the loci of its resultant probable circle centers are inside the region (P_x-maxR: P_x+maxR, P_y -maxR: P_y +maxR).

- Make a matrix[0: MaxR2, 0:MaxR2] which has location of all edge pixels and after that calculate the distances from the center to all the matrix points in order to make a radius map of radius, monitored by removing radii that do not lie within the range.Whereas MaxR2 is twice of the maximum radius.
- Increase the resultant components in the hough array for every edge pixel.
- Accumulate circles.

Syntax: (c_x c_y r)

Clear pixels which are less than $2\pi r$*(ratio)

- Remove alike circles.
- Draw circles on the original image.

The required results are not achieved by using CHT. So, another method is proposed to get required results.

3.3 Method 2: Histogram Based Edge Detection

Figure illustrates the block diagram of the proposed technique:

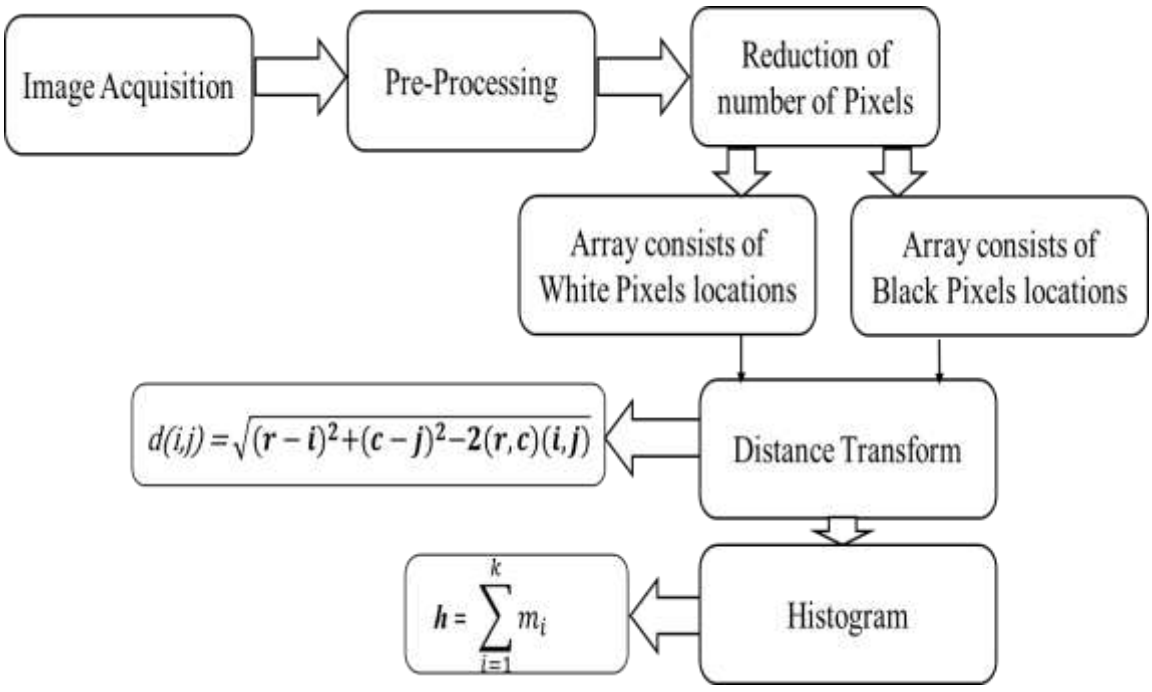

Figure 3.3: Algorithm of Proposed Methodology. Working of algorithm has shown in this figure.

Pixels in the perimeter of the circle can take an interest in the circle detection the pixels. These pixels take interest to the accumulator space by a set of votes around its area with a radius

equivalent to the circle being sought in CHT whereas the pixels that do not lie in the perimeter of the circle do not contribute in the procedure of the circle detection and consequently the initial step of this technique is to diminish the quantity of pixels in the picture to those which will take an interest decidedly in the identification procedure. This is accomplished by searching the edge identification of the image. To find the gradient G of the input image the Sobel Edge Detector has been used. The image is convolved with the Sobel operator that is a set of two 3x3 filter so as to detect the derivatives in both directions of the captured image(x-direction and y-direction).

Value of threshold is fixed to change the output image of edge detector into a binary image as the pixels having value one depict background and the pixels having value zero shows edges in the image which are greater than the set threshold. Distance transform has been applied after the identification of edge pixels.

$$d(u,v) = \sqrt{(p-x)^2 + (q-y)^2} \tag{3.1}$$

The distances between any pixel *(x,y)* and all edge pixels *(p,q)* are stored in a vector *d(u,v)*. Locations of edge pixels are stored in *(p,q)* vectors and locations of remaining pixels of an image are stored in *(x,y)* vectors. For each vector *d (u,v)* a histogram vector *h* is calculated.

$$h = \sum_{i=1}^{k} m_i \tag{3.2}$$

m_i in above equation is a function that is used to count the number of occurrences of a number in an image. The histogram for every vector *d(u,v)* illustrates the frequency of the pixel distances between the pixel (x_i,y_j) and all the edge pixels(p_i,q_j) . Then accumulator space is created from the number of pixels as votes which share the equivalent distance from (x_i,y_j). This procedure is repeated for every pixel (x_i,y_j) in the image to get an accumulator space.

Once the distances for entire edge pixels are acquired and stored in form of array, every pixel in the image is used to contribute in the voting method of the accumulator space as shown in Fig. 2. The distance which is calculated more repeatedly is used as the vote. Every vote in the accumulator space in Fig. 3 has the value of the number of edge pixels that share the same distance to the pixel location of the vote. Since this method is based on the histogram of the distances between pixels, it automatically determines the sizes of the circles it detects and no prior information is needed to be given to the algorithm in order to determine size. This makes our proposed method scale invariant in addition to that circle detection is orientation invariant.

Every pixel in the picture is utilized to partake in the voting methodology of the gatherer space by finding the separations to all the edge pixels in Fig. 2. The separation that is tallied all the more much of the time is utilized as the vote. Every vote in the collector space in Fig. 3 has the estimation of the quantity of edge pixels that have a similar separation to the pixel area of the vote. Since this strategy depends on the histogram of the separations between pixels, it naturally decides the sizes of the circles it recognizes and no earlier data is should have been given to the calculation with a specific end goal to decide estimate. This makes our proposed strategy scale invariant notwithstanding that circle discovery is introduction invariant

The purpose of histogram demonstration here, is to simplify the explanation of methodology under use. Here, the participation of histograms in the voting process and building of accumulator space can be clearly seen. It helps in showing the frequency count of distances between any random pixel and the pixels of the image which form the images. It is quite clear that they are spread at various distances. The value of number of edge pixels which are equidistant from the vote, is known to every vote in the accumulator space. Automatic determination of circle's sizes is made possible with the help of distance histogram. Therefore, the algorithm does not require prior information to calculate the size of the circle. This particular feature makes the proposed method independent of scale and orientation.

CHAPTER 4: RESULTS AND ANALYSIS

Results acquired using method 1 are shown below.

4.1 Method 1: Circular Hough Transform

1. Read the original image

Figure 4.1: Original Image

2. Gray Scale Image-Processing:

The image acquisition DSLR camera is the digital image, the image model is RGB space model, namely Red, Green and Blue. RGB system is through change of the intensity ratios of R, G, B to get different color.

$$C = rR+gG+bB$$

Wherein, C represents a certain color, R, G, B on behalf of tricolor, and R, G, B representing the proportion coefficient, and r+b+g=1[Hendra Prima Syahputra, Tae Jo Ko.,2013]. In order to simplify the later operation process, need to gray image processing, generate a special image which R=G=B, through the RGB three-dimensional space to one-dimensional space mapping relationship between gray to gray image processing. The results is shown in Figure.

Figure 4.2: Gray Image

3. Compute gradient magnitude and gradient direction using Sobel's gradient operator.

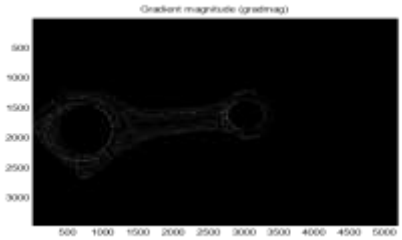

Figure 4.3: Gradient Magnitude

4. Image is converted into binary image for further processing.

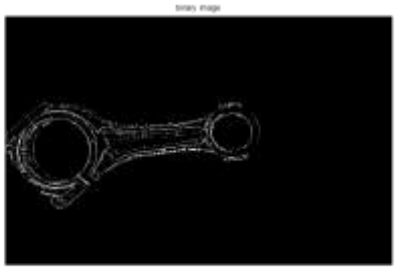

Figure 4.4: Binary Image

5. Image filtering process: There is a noise in an image, so need to find a way which can eliminate the noise, but also can ensure the integrity of the filtering means the details of images.

Median filter is a nonlinear filter, it will be the gray value of each pixel which is set for all pixels of the points of a median neighbourhood within the window, thereby eliminating the isolated noise points. This method is essentially a two-dimensional array of filter, the filter window is two-dimensional. Two dimensional median filter output:

$$g(x,y) = \text{med}\{f(x-k, y-1), (k, 1 \in W)\} \quad (4.1)$$

Among them, f (x, y), g (x, y) were the original image and the processing image. W is 2D template which is usually divided of 3*3, 5*5, 7*7 region, also can be different shapes, such as linear, square, circular, the figure ten and the circular etc. This algorithm selects the input image which pixel is related to 3*3, 5*5, 7*7. Result of connecting-rod is shown in figure:

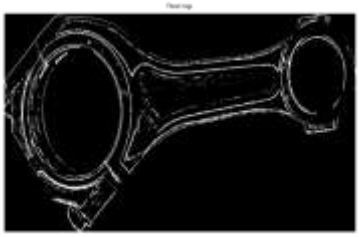

Figure 4.5: Filtered Image

6. Image is cropped autonomously due to its large size.

Syntax:

```
% Get all rows and columns where the image is nonzero
[nonZeroRows nonZeroColumns] = find(grayImage);
% Get the cropping parameters
topRow = min(nonZeroRows(:));
bottomRow = max(nonZeroRows(:));
leftColumn = min(nonZeroColumns(:));
rightColumn = max(nonZeroColumns(:));
% Extract a cropped image from the original.
croppedImage = grayImage(topRow:bottomRow, leftColumn:rightColumn);
% Display the original gray scale image.
imshow(croppedImage, []);
title('Cropped Grayscale Image', 'FontSize', fontSize);
```

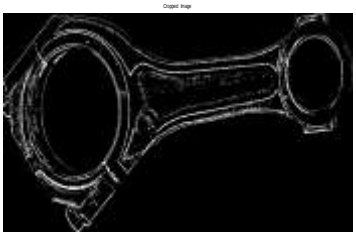

Figure 4.6: Cropped Image

7. Bwareaopen command is used to remove pixels below than 3000 so that crescent get disappear from the image.

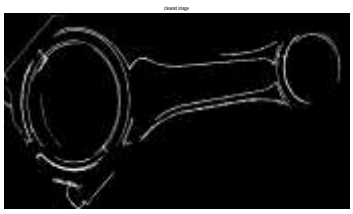

Figure 4.7: Cleaned Image

8. Circles are detected.

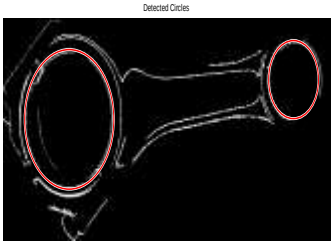

Figure 4.8: Detected Circles

Table 4-1 shows total number of connecting-rods, their code, total number of images and total number of orientations in which connecting-rods are placed to take images.

Table 4-1: Number of Connecting-rods, Codes, Number of Images and Total Number of Positions

No of Connecting-rods	Codes	No. of images	Total No. of Positions
C1	EG2945	50	5
C2	DF2444	50	5
C3	EG39	50	5
C4	EG2945	50	5
C5	DF2444	50	5
C6	EG39	50	5

The table 4-2, table 4-3 and table 4-4 for C1, C2 and C3 are shown below where LC stands for large and SC stands for smaller circle. All images were captured from fixed height by keeping the lighting conditions same and acquired the results.

C1:

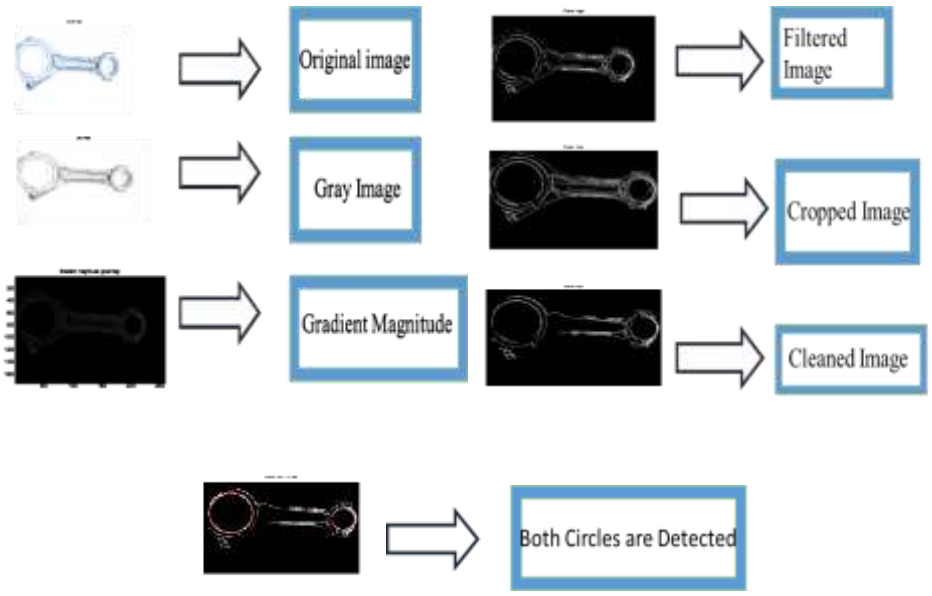

Figure 4.9: RGB Image of Rod C1, Intermediate Pre-processing Stages and illustrates circle detection for C1

Table 4-2: Centers of Large bore and Small Bore for C1 and its Radius using CHT

S.No.	Centers of Large Bore and Small Bore		Radius
1.	LC = 408.3973	117.4506	LC = 65.561
	SC = 78.5978	98.1399	SC = 46
2.	LC = 408.9692	117.4110	LC = 65.561
	SC = 78.1271	97.6502	SC = 46
3.	LC = 408.9692	117.4110	LC = 65.561
	SC = 78.1271	97.6502	SC = 46
4.	LC = 408.6687	117.3953	LC = 62.015
	SC = 79.5818	97.5511	SC = 35
5.	LC = 408.6687	117.3953	LC = 62.015
	SC = 79.5818	97.5511	SC = 35
6.	LC = 408.6202	117.5470	LC = 66.473
	SC = 78.3344	98.3825	SC = 47
7.	LC = 408.9692	117.4110	LC = 65.561
	SC = 78.1271	97.6502	SC = 46

It can be seen from the table that for given images the radii of both circles vary every time when processed.

C2:

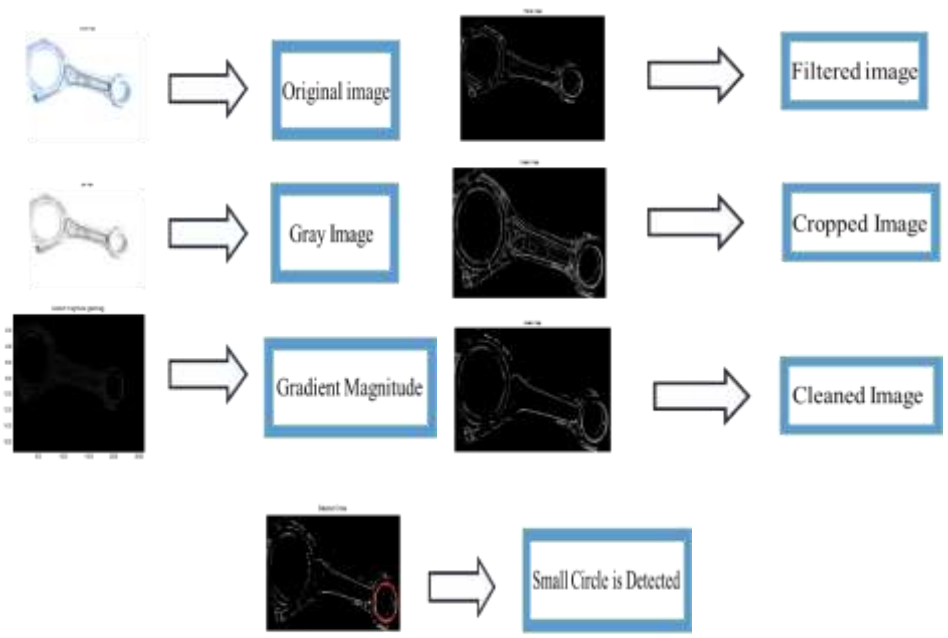

Figure 4.10: RGB Image of Rod C2, Intermediate Pre-processing Stages and illustrates circle detection for C2

Table 4-3: Centers of Large bore and Small Bore for C2 and its Radius using CHT

S.No.	Centers of Large Bore and Small Bore		Radius
1.	SC = 438.8097	157.7509	35
2.	SC = 437.9193	157. 9610	47
3.	SC = 437.9193	157. 9610	46
4.	SC = 439.2133	157.1380	34
5.	SC = 439.2133	157.1380	34
6.	SC = 430.6142	156.3884	46
7.	SC = 438.8097	157.7509	35

Same steps were followed for the circle detection for all rods. However it is evident from the image, that only one of the two circles is detected.

C3:

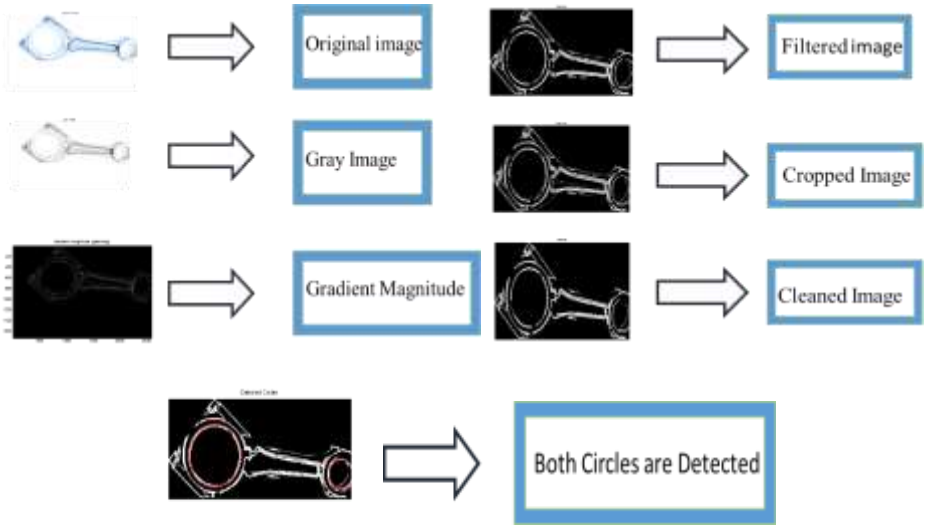

Figure 4.11: RGB Image of Rod C3, Intermediate Pre-processing Stages and illustrates circle detection for C3

Table 4-4: Centers of Large bore and Small Bore for C3 and its Diameter using CHT

S.No.	Centers of Large Bore and Small Bore		Radius
1.	LC = 399.0845	170.3376	LC = 62.015
	SC = 76.4989	100.9715	SC = 35
2.	LC = 399.0845	170.3376	LC = 62.015
	SC = 76.4989	100.9715	SC = 35
3.	LC = 399.0845	170.3376	LC = 62.015
	SC = 76.4989	100.9715	SC = 35
4.	LC = 399.0743	170.3470	LC = 67.528
	SC = 76.3810	100.8429	SC = 34
5.	LC = 399.2789	170.3472	LC = 66.097
	SC = 76.2739	100.9264	SC = 38
6.	LC = 399.2540	170.2738	LC = 67.256
	SC = 76.4329	100.6914	SC = 32
7.	LC = 399.0230	170.3041	LC = 60.456
	SC = 76.2798	100.6201	SC = 37

The results show that it is also possible, that for some rods, sometimes the radii are same while the other times, they are not.

Where accuracy is not the main priority, CHT proves to be helpful and can be employed. But, where accuracy is a priority, CHT is not the best algorithm to use.

The results of CHT depict that the shape of circles are being perfectly detected but since it compromises accuracy, it does not give the same result for every image which are taken from fixed height by keeping the lightning conditions same, which it should.

According to the adopted scale **1 pixel = 0.11mm**. Having said that, running CHT yields a result that exceeds the tolerance level, since a variation of **4 to 5 pixels** is observed every time while finding radius. The given tolerance range is **+0.007mm** for diameters of both circles of Connecting-rod. Therefore, this variation goes far beyond the acceptable range.

In addition to that, CHT is not at all feasible to be applied in real time due to the need for altering methods for every image i.e either it will be edge threshold or phase code. To detect circles of different sizes, one would have to use different methods for each image, which gets tedious and impractical.

4.2 Method 2: Histogram Based Edge Detection

The method that is proposed, starts with acquisition of image, then comes the pre-processing that is already explained. Next step is the autonomous reduction of pixels. Then there are two vectors which stores the locations of white and black pixels, separately. Once the edge pixels have been identified distance transform is applied.

C1:

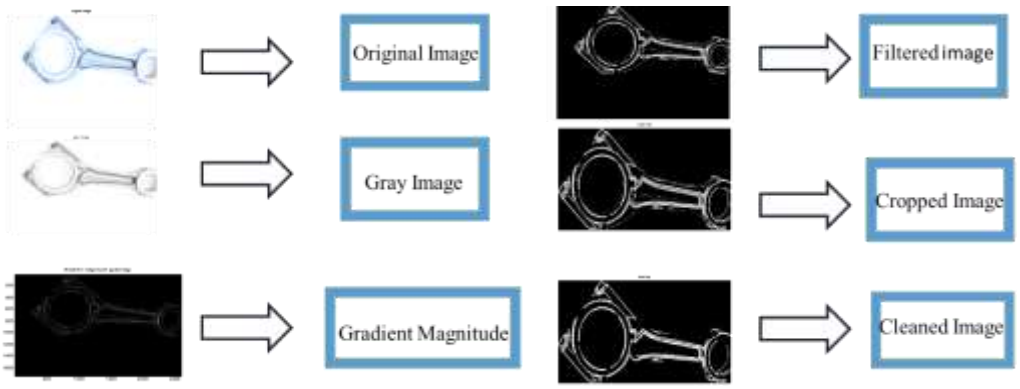

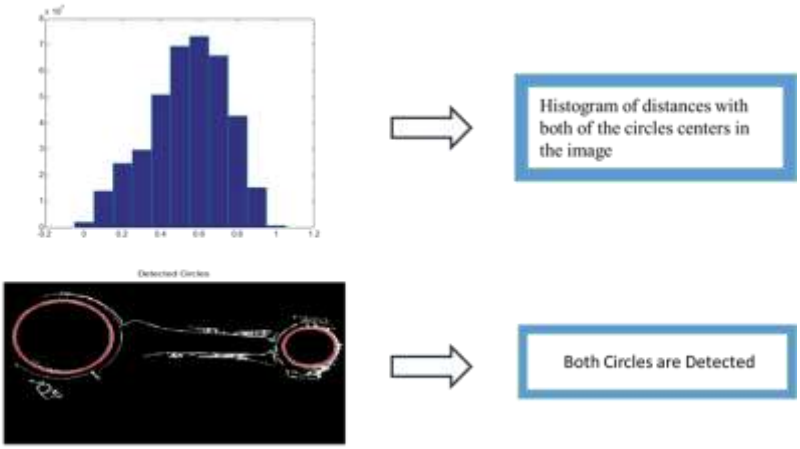

Figure 4.12: Histogram Based Edge Detection and Circle Detection for C1

Table 4-5: Centers of Large bore and Small Bore for C1 and radii using HBED

S.No.	Center		Radius
1.	LC = 118.6228	118.9006	LC = 62.015
	SC = 438.8097	157.7509	SC = 35
2.	LC = 118.6228	118.9006	LC = 62.015
	SC = 438.8097	157.7509	SC = 35
3.	LC = 118.6228	118.9006	LC = 62.015
	SC = 438.8097	157.7509	SC = 35
4.	LC = 118.6228	118.9006	LC = 62.015
	SC = 438.8097	157.7509	SC = 35
5.	LC = 118.6228	118.9006	LC = 62.015
	SC = 438.8097	157.7509	SC = 35
6.	LC = 118.6228	118.9006	LC = 62.015
	SC = 438.8097	157.7509	SC = 35
7.	LC = 118.6228	118.9006	LC = 62.015
	SC = 438.8097	157.7509	SC = 35

The radii computed using the algorithm are all identical.

Table 4-6: Measured Diameters and Actual Diameters for C1

S.No.	Measured Diameter	Actual Diameter
1.	LC = 67.420	LC = 67.420+0.007
	SC = 38.015	SC =38.015+0.007
2.	LC = 67.420	LC = 67.420+0.007
	SC = 38.015	SC =38.015+0.007
3.	LC = 67.420	LC = 67.420+0.007
	SC = 38.015	SC =38.015+0.007
4.	LC = 67.420	LC = 67.420+0.007
	SC = 38.015	SC =38.015+0.007
5.	LC = 67.420	LC = 67.420+0.007
	SC = 38.015	SC =38.015+0.007
6.	LC = 67.420	LC = 67.420+0.007
	SC = 38.015	SC =38.015+0.007
7.	LC = 67.420	LC = 67.420+0.007
	SC = 38.015	SC =38.015+0.007

Table 4-6 shows a comparison between the calculated and actual diameter.

If we take images after changing the position of connecting rod it only changes the centers of the connecting-rod while their radii are kept same. The results after changing the position of connecting-rod are shown below:

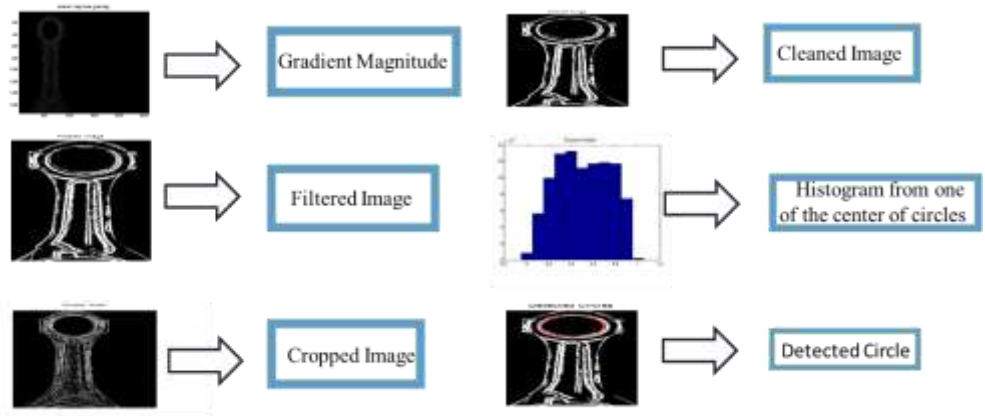

Figure 4.13: Histogram Based Edge Detection and Circle Detection for C1 with different position

Table 4-7: Center of Small Bore for C1 and its Radius using HBED

S. No.	Center		Radius
1.	SC = 76.1406	53.8903	SC = 35
2.	SC = 76.1406	53.8903	SC = 35
3.	SC = 76.1406	53.8903	SC = 35
4.	SC = 76.1406	53.8903	SC = 35
5.	SC = 76.1406	53.8903	SC = 35
6.	SC = 76.1406	53.8903	SC = 35
7.	SC = 76.1406	53.8903	SC = 35

Table 4-8: Measured Diameter and Actual Diameter for C1

S. No.	Measured Diameter	Actual Diameter
1	SC = 38.015	SC =38.015+0.007
2	SC = 38.015	SC =38.015+0.007
4	SC = 38.015	SC =38.015+0.007
5	SC = 38.015	SC =38.015+0.007
6	SC = 38.015	SC =38.015+0.007
7	SC = 38.015	SC =38.015+0.007

C2:

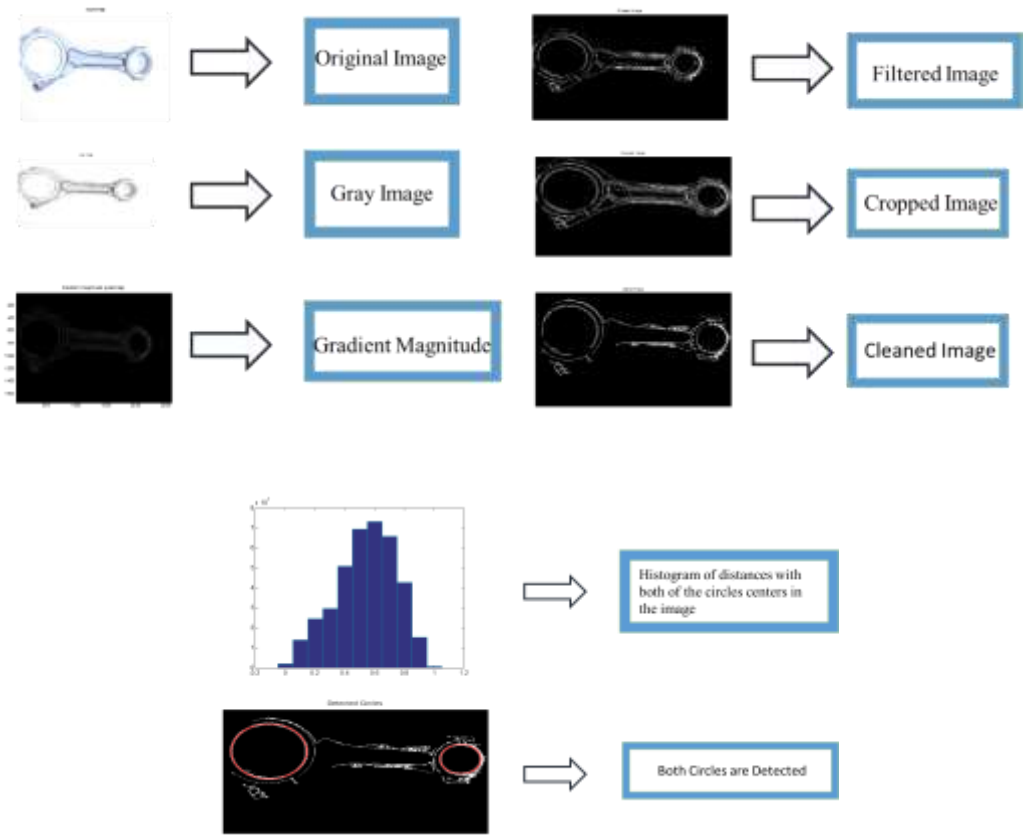

Figure 4.14: Histogram Based Edge Detection and Circle Detection for C2

Table 4-9: Centers of Large bore and Small Bore for C2 and its radii using HBED

S.No.	Centers of Large Bore and Small Bore		Radius
1.	LC = 408.6687	117.3953	LC = 62.015
	SC = 79.5818	97.5511	SC = 35
2.	LC = 408.6687	117.3953	LC = 62.015
	SC = 79.5818	97.5511	SC = 35
3.	LC = 408.6687	117.3953	LC = 62.015
	SC = 79.5818	97.5511	SC = 35
4.	LC = 408.6687	117.3953	LC = 62.015
	SC = 79.5818	97.5511	SC = 35
5.	LC = 408.6687	117.3953	LC = 62.015
	SC = 79.5818	97.5511	SC = 35
6.	LC = 408.6687	117.3953	LC = 62.015
	SC = 79.5818	97.5511	SC = 35
7.	LC = 408.6687	117.3953	LC = 62.015
	SC = 79.5818	97.5511	SC = 35

Table 4-10: Measured Diameters and Actual Diameters for C2

S.No.	Measured Diameter	Actual Diameter
1.	LC = 67.420	LC = 67.420+0.007
	SC = 38.015	SC =38.015+0.007
2.	LC = 67.420	LC = 67.420+0.007
	SC = 38.015	SC =38.015+0.007
3.	LC = 67.420	LC = 67.420+0.007
	SC = 38.015	SC =38.015+0.007
4.	LC = 67.420	LC = 67.420+0.007
	SC = 38.015	SC =38.015+0.007
5.	LC = 67.420	LC = 67.420+0.007
	SC = 38.015	SC =38.015+0.007
6.	LC = 67.420	LC = 67.420+0.007
	SC = 38.015	SC =38.015+0.007
7.	LC = 67.420	LC = 67.420+0.007
	SC = 38.015	SC =38.015+0.007

C3:

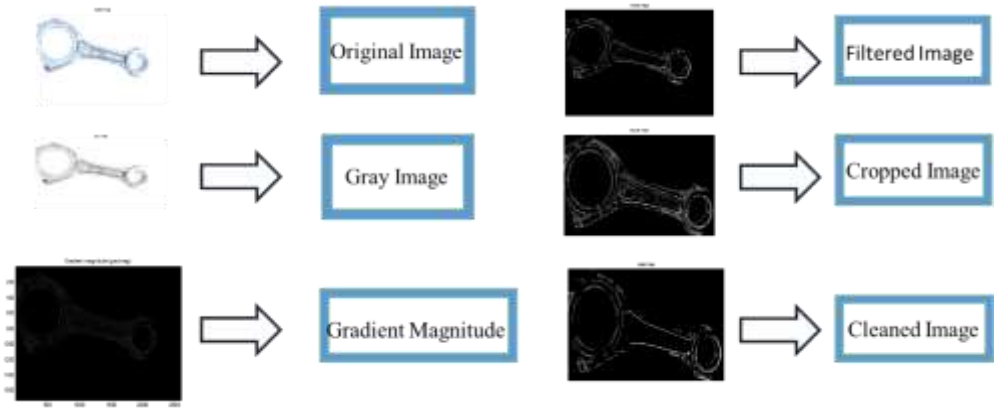

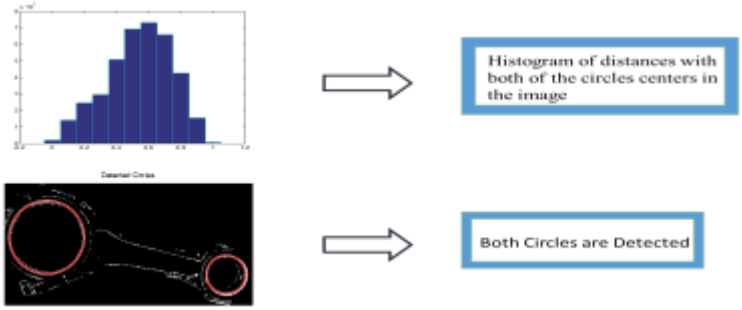

Figure 4.15: Histogram Based Edge Detection and Circle Detection for C3

Table 4-11: Centers of Large Bore and Small Bore and its Radii for C3 using HBED

S.No.	Centers of Large Bore and Small Bore		Radius
1.	LC = 399.0845	170.3376	LC = 62.015
	SC = 76.4989	100.9715	SC = 35
2.	LC = 399.0845	170.3376	LC = 62.015
	SC = 76.4989	100.9715	SC = 35
3.	LC = 399.0845	170.3376	LC = 62.015
	SC = 76.4989	100.9715	SC = 35
4.	LC = 399.0845	170.3376	LC = 62.015
	SC = 76.4989	100.9715	SC = 35
5.	LC = 399.0845	170.3376	LC = 62.015
	SC = 76.4989	100.9715	SC = 35
6.	LC = 399.0845	170.3376	LC = 62.015
	SC = 76.4989	100.9715	SC = 35
7.	LC = 399.0845	170.3376	LC = 62.015
	SC = 76.4989	100.9715	SC = 35

Table 4-12: Measured Diameters and Actual Diameters for C3

S.No.	Measured Diameter	Actual Diameter
1.	LC = 67.420	LC = 67.420+0.007
	SC = 38.015	SC =38.015+0.007
2.	LC = 67.420	LC = 67.420+0.007
	SC = 38.015	SC =38.015+0.007
3.	LC = 67.420	LC = 67.420+0.007
	SC = 38.015	SC =38.015+0.007
4.	LC = 67.420	LC = 67.420+0.007
	SC = 38.015	SC =38.015+0.007
5.	LC = 67.420	LC = 67.420+0.007
	SC = 38.015	SC =38.015+0.007
6.	LC = 67.420	LC = 67.420+0.007
	SC = 38.015	SC =38.015+0.007
7.	LC = 67.420	LC = 67.420+0.007
	SC = 38.015	SC =38.015+0.007

Algorithm proposed is implemented on the number of images in which connecting rods are kept in distinct positions. For every position desired results have been achieved, like detection of both circles and diameter of each circle in a provided image. This system is not orientation dependent. Table and table show that position of the rod affects the center but not the radius or diameter.

4.3 Quality Inspection System

Quality inspection system comes into play when we have to separate the OK component from the Not OK-components. The Not OK components are further classified in two groups: the oversized and undersized.

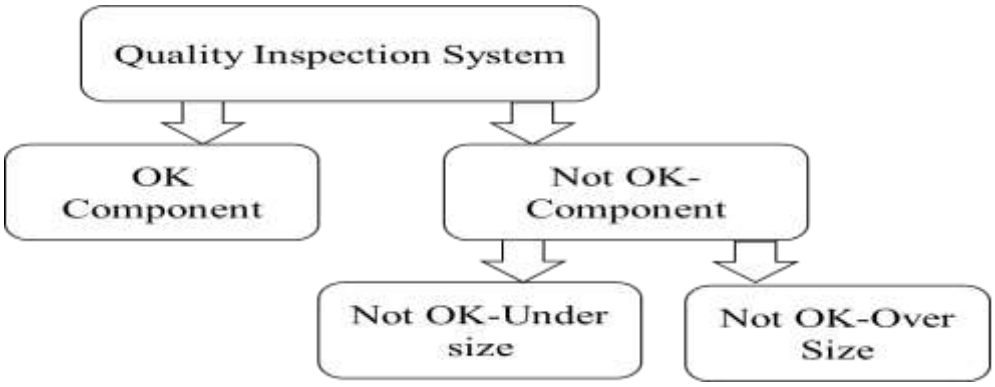

Figure 4.16: Quality Inspection System for Connecting-Rod

Out of the dataset of 300 images of connecting-rods including defected connecting-rods taken before have been tested using developed quality inspection system and results are shown below.

Table 4-13: Measured Diameters, Actual Diameters and Status of all 6 Connecting-rods.

S.No.	Measured Diameter (C1, C2, C3, C4, C5,C6)	Actual Diameter (C1, C2, C3, C4,C5, C6)	Status
1.	LC = 76.0298	LC = 67.420+0.007	Not OK-Over size
	SC = 43.4456	SC =38.015+0.007	
2.	LC = 67.420	LC = 67.420+0.007	OK
	SC = 38.015	SC =38.015+0.007	
3.	LC = 67.420	LC = 67.420+0.007	OK
	SC = 38.015	SC =38.015+0.007	
4.	LC = 56.47	LC = 67.420+0.007	Not OK-Under size
	SC = 34.75	SC =38.015+0.007	
5.	LC = 76.0298	LC = 67.420+0.007	Not OK-Over size
	SC = 43.4456	SC =38.015+0.007	
6.	LC = 54.307	LC = 67.420+0.007	Not OK-Undersize
	SC = 34.7564	SC =38.015+0.007	
7.	LC = 67.420	LC = 67.420+0.007	Ok
	SC = 38.015	SC =38.015+0.007	
8.	LC = 56.47	LC = 67.420+0.007	Not OK-Undersize
	SC = 34.75	SC =38.015+0.007	
9.	LC = 54.307	LC = 67.420+0.007	Not OK-Undersize
	SC = 34.7564	SC =38.015+0.007	
10.	LC = 67.420	LC = 67.420+0.007	OK
	SC = 38.015	SC =38.015+0.007	
11.	LC = 76.0298	LC = 67.420+0.007	Not OK-Over size
	SC = 43.4456	SC =38.015+0.007	
12.	LC = 56.47	LC = 67.420+0.007	Not Ok-Under size
	SC = 34.75	SC =38.015+0.007	
13.	LC = 67.420	LC = 67.420+0.007	OK
	SC = 38.015	SC =38.015+0.007	

For the defective rods, the proposed system has divided them in two categories for example undersized and oversized. The algorithm was run on a dataset of 300 images and results were found to be 98% accurate. 2% inaccuracy in results were found due to pixels variation. This pixel variation was about 1 to 2 pixels.

In recent times, machines have started to replace human labour, to a great extent. Now, the number of people required to do the same work, is greatly reduced due to the mechanical revolution which has taken our industries by a storm.

When it comes to production, the worst thing for a company's reputation, is inconsistency in its production. The risk of inconsistency increases when the products are being produced by different hands and then examined by different eyes.

Induction of machines at both of these stages, is a measure which prevents inconsistency.

In addition to this, a machine, contrary to human who normally works 8 hours per day, can work tirelessly, for 24 hours a day. In this case machine is programmed and thus run without needing any input from human being. All that is required, is an operator. If a factory desires to produce big, whether to merely improve their output or to meet a deadline, they can make the machine operators and technicians take shifts while the rest of the job is done by the system.

S. No.	Machine Vision System Component	COST (Rs)
1	Computer System(Dell Optiplex 7040MT Core i7)	77000
2	Software(MATLAB)	1,25,000
3	DSLR Camera	74000
	Total Cost	2,76,000

The estimated cost of proposed machine system is 2, 76,000. The system does not need to be paid a salary. It does not require allowance like human beings to work in extra hours which makes it very cost-effective. Not only this, a machine is capable of performing task at rate much great than that of a human which makes thing more efficient in terms of cost and time as well.

CHAPTER 5: CONCLUSION

In this project, a machine vision based quality inspection system for Connecting-rod has been described. The proposed system executes dimensional computations having critical lengths on Connecting-rods. The prototype for the computations and the logical development for improvement of errors have been explained. The demonstrated analytical system is efficient and also perfectly satisfies the terms of the industrial quality production control system. Additionally, this solution has affected an extreme decrease of manufacturing waste as a constant monitoring of production processes can ensure that there are not faulty pieces being made which will eventually lead the prevention of the production of wastage of material. Lesser cost required to built-up the proposed system as compared to existing manual systems.

CHAPTER 6: LIMITATIONS AND RECOMMENDATIONS

High resolution lens is needed as webcams and other digital cameras give variation of 50 to 100 pixels which is not acceptable. DSLR is a must to get accurate results, a video camera of high resolution can be used. The simulation of algorithm was done on stand-alone images. This algorithm can only be used to measure the diameters of connecting-rods, not other parameters. Its efficiency is dependent on the processing time. For this project, results are acquired using processor of i7core and 8gb RAM. The proposed algorithm is robust and is able to identify incomplete obstructed circles, still, the computation time of this method is 2 to 3 minutes to get required results which can be ruled out using faster processor. Optical sensors can be used to accurately determine the positions of connecting-rods while they move on the conveyor belt, one after the other.

REFERNCES

[1] G. Di Leo, C. Liguori, A. Paolillo and A. Pietrosanto, "Machine vision systems for on line quality monitoring in industrial applications", *ACTA IMEKO*, vol. 4, no. 1, p. 121, 2015.

[2] G. Di Leo, C. Linguori, E. Adiutori and F. Promutico, "Online Visual Inspection of Defects in the Assembly of Electromechanical Parts", in *Instrumentation and Measurement Technology Conference(IM2TC)*, 2014.

[3] A. Pereira, M. Reis and P. Saraiva, "Quality Control of Food Products using Image Analysis and Multivariate Statistical Tools", *Industrial & Engineering Chemistry Research*, vol. 48, no. 2, pp. 988-998, 2009.

[4] S.Sathiyamoorthy ., "INDUSTRIAL APPLICATION OF MACHINE VISION", *International Journal of Research in Engineering and Technology*, vol. 03, no. 19, pp. 678-682, 2014.

[5] J. Canny, "A Computation Approach to Edge Detetction", in *Pattern Analysis And Machine Intelligence,IEEE Transactions*, 1986, pp. 679-98.

[6] R. Muthukrishnan and M. Radha, "Edge Detection Techniques For Image Segmentation", *International Journal of Computer Science and Information Technology*, vol. 3, no. 6, pp. 259-267, 2011.

[7] L. Sun, E. Zhao, L. Ma and L. Zheng, "An Edge Detection Method Based on Improved Sobel Operator", *Advanced Materials Research*, vol. 971-973, pp. 1529-1532, 2014.

[8] P. Patidar, M. Gupta, S. Srivastava and A. Nagawat, "Image De-noising by Various Filters for Different Noise", *International Journal of Computer Applications*, vol. 9, no. 4, pp. 45-50, 2010.

[9] J. C.Church, Y. Chen and S. V.Rice, "A Spatial Median Filter for Noise Removal in Digital Images", in *Southeastcon,2008.IEEE*, 2008.

[10] N. Dwibedi and N. Panda, "IMAGE DEBLURRING WITH WEINER HOFF FILTER WITH THE ESTIMATION OF PSF PARAMETER", *Journal of Technological Advances and Scientific Research*, vol. 1, no. 3, pp. 154-160, 2015.

[11] S. Kaur and S. Kaur, "An Efficient Method of Number Plate Extraction from Indian Vehicles Image", *International Journal of Computer Applications*, vol. 88, no. 4, pp. 14-19, 2014.

[12] L. Li, S. Li and H. Zhu, "An Efficient Scehme for Detecting Copy-move Forged Images by Local Binary Patterns", *Journal of Information Hiding and Multimedia Signal Processing*, vol. 4, no. 2071-4212, p. 1, 2013.

[13] S. Kent, O. Ocan and T. Ensari, "Speckle Reduction of Synthetic Aperture Radar Images Using Wavelet Filtering", in *ITG,VDE,FGAN,DLR,EADS, astrium.EUSAR 2004 Proceedings,5th European Conference on Synthetic Aperture Radar*, Germany, 2004.

[14] S. Lim, N. Mat Isa, C. Ooi and K. Toh, "A new histogram equalization method for digital image enhancement and brightness preservation", *Signal, Image and Video Processing*, vol. 9, no. 3, pp. 675-689, 2013.

[15] R. Deb, D. Sengupta, R. Das, S. Mahajan and S. Mitra, "Development of an Image Enhancement Method and a GUI", *International Journal of Signal Processing, Image Processing and Pattern Recognition*, vol. 8, no. 6, pp. 227-234, 2015.

[16] R. C.Gonzalez and R. .E Woods, *Digital Image Processing*, 2nd ed. 2002.

[17] R. Singh and M. Dixit, "Histogram Equalization: A Strong Technique for Image Enhancement", *International Journal of Signal Processing, Image Processing and Pattern Recognition*, vol. 8, no. 8, pp. 345-352, 2015.

[18] J. Kaur and A. Sharma, "Review Paper on Edge Detection Techniques in Digital Image Processing", in *7th International Conference on Innovative Research in Engineering Science and Management(ICIRESM-16)*, Delhi, 2016.

[19] M. Sonka, R. Boyle and V. Hlavac, *Image processing, analysis and machine vision*, 1st ed. Kluwer Academic Publishers, 1993.

[20] S. Sarangi, S. Sabut and D. Majhi, "Evaluation and comparison of retinal blood vessels extraction using edge detectors in diabetic retinopathy", *International Journal of Signal and Imaging Systems Engineering*, vol. 9, no. 3, p. 174, 2016.

[21] S. Israni and S. Jain, "Edge Detection of License Plate Using Sobel Operator", in *Electrical,Electronics and Optimization Techniques(ICEEOT), International Conference*

on, 2016.

[22] K. Kalyan, S. Jain, R. Lele, M. Joshi and A. Chowdhary, "Application of Artificial Neural Networks towards the Determination of Presence of Disease Condition in Ultra Sound Images of Kidney", *International Journal of Computer Engineering & Technology*, vol. 4, no. 5, pp. 232-243, 2013.

[23] A. M.phil Scholar, "Object Detection In Image Processing Using Edge Detection Techniques", *IOSR Journal of Engineering*, vol. 4, no. 3, pp. 10-13, 2014.

[24] D. Shen, X. E and L. Zhang, "Application of Improved Sobel Algorithm in Medical Image Edge Detection", *Applied Mechanics and Materials*, vol. 678, pp. 151-154, 2014.

[25] K. Jena, "Results Analysis of Different Images Edges by Applying Existing & New Techniques'", *International Journal of Computer Science & Information Technology and Security*, vol. 5, no. 1, 2015.

[26] J. Mizera-Pietraszko and S. Grabowski, "PORE algorithm for object recognition in photo layers based on parametric characteristics of the object edges", in *Innovative Computing Technology(INTECH), 2016 Sixth International Conference on*, 2016.

[27] P. Nguyen, J. Cho and S. Cho, "An architecture for real-time hardware co-simulation of edge detection in image processing using Prewitt edge operator", in *Electronics,Information and Communications (ICEIC), 2014 International Conference on*, 2014.

[28] Z. Weipeng, "Measuring Method for Diameter of Bearings Based on the Edge Detection Using Zernike Moment", *The Open Automation and Control Systems Journal*, vol. 7, no. 1, pp. 112-117, 2015.

[29] G. C.R. and H. D. Giriprakash, "Image Steganography by Variable Embedding and Multiple Edge Detection using Canny Operator", *International Journal of Computer Applications*, vol. 48, no. 16, pp. 15-19, 2012.

[30] Z. Zhang, S. Zhang and Q. Li, "Robust and Accurate Vision-Based Pose Estimation Algorithm Based on Four Coplanar Feature Points", *Sensors*, vol. 16, no. 12, p. 2173, 2016.

[31] Y. Zhao, H. Pan, C. Du and Y. Zheng, "Principal direction-based Hough transform for line detection", *Optical Review*, vol. 22, no. 2, pp. 224-231, 2015.

[32] T. Aung and M. Zaw, "Video Based Lane Departure Warning System using Hough TransformThandar", *Internationa Journal of Scientific Engineering and Technology Research*, vol. 3, no. 13, pp. 2955-2960, 2014.

[33] X. Wang, H. Tan, F. Zhou and Y. Zhao, "Real Time Classified Hough Transform Line Detection Based on FPGA", in *5th International Conference on Computer Sciences ad Automation Engineering(ICCSAE)*, 2015.

[34] L. Fernandes and M. Oliveira, "Real-time line detection through an improved Hough transform voting scheme", *Pattern Recognition*, vol. 41, no. 1, pp. 299-314, 2008.

[35] Zhong-Ho Chen, A. Su and Ming-Ting Sun, "Resource-Efficient FPGA Architecture and Implementation of Hough Transform", *IEEE Transactions on Very Large Scale Integration (VLSI) Systems*, vol. 20, no. 8, pp. 1419-1428, 2012.

[36] M. Wu, Z. Song, B. Li, F. Li, B. Li and C. Shen, "A method to Detect Circle Based on Hough Transform", in *International Conference on Information Sciences ,Machinery,Materials and Energy(ICISMME)*, 2015.

[37] G. Damaryam, "A Hough Transform Implementation for Line Detection for a Mobile Robot Self-Navigation System", *IOSR Journal of Computer Engineering (IOSR-JCE)*, vol. 17, no. 6, pp. 33-44, 2015.

[38] T. Wei, Y. Lu, X. Li and J. Liu, "Web Page Segmentation based on Hough Transform and Vision Cues", in *Signal and Information Processing Association Annual Summit and Conference (APSIPA), 2015 Asia-Pacific*, 2016.

[39] J. Cho, Y. Jang and S. Cho, "Lane Recognition Algorithm Using Hough Transform with Apllied Accumulator cells in Multi-Channel ROY", in *Consumer Electronics(ISCE), The 18th IEEE International Symposium on*, 2014.

[40] H. Oliveira and P. Correia, "CrackIT â€" An image processing toolbox for crack detection and characterization", in *Image Processing (ICIP), 2014 IEEE International Conference on*, 2014.

[41] R. Gozalez, R. Woods and S. Eddins, *Representation and Description in Digital Image Processing using MATLAB*, 3rd ed. Haryana: Tata McGraw Hill Education Private Limited, 2010.

[42] O. Marques, *Practical image and video processing using MATLAB*, 1st ed. Hoboken, N.J.: John Wiley, 2011.

[43] "The Mathworks.Inc.,", 2015. [Online]. Available: http://in.mathworks.com/product/imaq. [Accessed: 28- Feb- 2017].

[44] J. Semmlow, *Biosignal and medical image processing*, 1st ed. [Place of publication not identified]: Crc Press, 2014.

[45] S. Awaida, "Automatic Check Digits Recognition for Arabic Using Multi-Scale Features, HMM and SVM Classifiers", *British Journal of Mathematics & Computer Science*, vol. 4, no. 17, pp. 2521-2535, 2014.

[46] L. Croft, P. Goodwill, J. Konkle, H. Arami, D. Price, A. LI, E. Saritas and S. Conolly, "Low drive field amplitude for improved image resolution in magnetic particle imaging", 2016.

[47] Weiming Dong, Ning Zhou, Tong-Yee Lee, Fuzhang Wu, Yan Kong and Xiaopeng Zhang, "Summarization-Based Image Resizing by Intelligent Object Carving", *IEEE Transactions on Visualization and Computer Graphics*, vol. 20, no. 1, pp. 1-1, 2014.

[48] Y. Yang, T. Geng, P. Li and W. Yang, "Research for On-Line Measurement of Optical Fiber Diameter Based on Machine Vision", *Advanced Materials Research*, vol. 433-440, pp. 6497-6502, 2012.

[49] Z. Zhang, Z. Chen, J. Shi, F. Jia and M. Dai, "Surface roughness vision measurement in different ambient light conditions", *International Journal of Computer Applications in Technology*, vol. 39, no. 123, p. 53, 2010.

[50] "Development of a Two-Level Segmentation System for Iris Recognition Using Circular and Linear Hough Transform Algorithm", *International Journal of Science and Research (IJSR)*, vol. 5, no. 2, pp. 1278-1286, 2016.

[51] A. Biswas and G. M.K, "Face Recognition Algorithm based on Orientation Histogram of Hough Peaks", *International Journal of Artificial Intelligence & Applications*, vol. 5, no. 5, pp. 107-114, 2014.

[52] A. Sewisy, "Graphical Techniques for Detecting Lines with the Hough Transform", *International Journal of Computer Mathematics*, vol. 79, no. 1, pp. 49-64, 2002.

[53] L. Jiang, "Fast detection of multi-circle with randomized Hough transform", *Optoelectronics Letters*, vol. 5, no. 5, pp. 397-400, 2009.